AD_____

Award Number: W81XWH-09-1-0409

TITLE: SYSTEMATIC INVESTIGATION OF KEY SURVIVAL AND GROWTH PATHWAYS IN BREAST CANCER

PRINCIPAL INVESTIGATOR: DR. JUNJIE CHEN

CONTRACTING ORGANIZATION: University of Texas M.D. Anderson Cancer Center
Houston, TX 77030

REPORT DATE: September 2011

TYPE OF REPORT: Annual

PREPARED FOR: U.S. Army Medical Research and Materiel Command
Fort Detrick, Maryland 21702-5012

# REPORT DOCUMENTATION PAGE

*Form Approved*
*OMB No. 0704-0188*



| 1. REPORT DATE *(DD-MM-YYYY)* | 2. REPORT TYPE | 3. DATES COVERED *(From - To)* |
|---|---|---|
| 01-09-2011 | Annual | 1 SEP 2010- 31 AUG 2011 |

**4. TITLE AND SUBTITLE**

SYSTEMATIC INVESTIGATION OF KEY SURVIVAL AND GROWTH PATHWAYS IN BREAST CANCER

**5a. CONTRACT NUMBER**

**5b. GRANT NUMBER**
W81XWH-09-1-0409

**5c. PROGRAM ELEMENT NUMBER**

**6. AUTHOR(S)**
DR. JUNJIE CHEN

E-Mail: jchen8@mdanderson.org

**5d. PROJECT NUMBER**

**5e. TASK NUMBER**

**5f. WORK UNIT NUMBER**

**7. PERFORMING ORGANIZATION NAME(S) AND ADDRESS(ES)**
University of Texas M.D. Anderson Cancer Center
Houston, TX 77030

**8. PERFORMING ORGANIZATION REPORT NUMBER**

**9. SPONSORING / MONITORING AGENCY NAME(S) AND ADDRESS(ES)**
U.S. Army Medical Research and Materiel Command
Fort Detrick, Maryland 21702-5012

**10. SPONSOR/MONITOR'S ACRONYM(S)**

**11. SPONSOR/MONITOR'S REPORT NUMBER(S)**

**12. DISTRIBUTION / AVAILABILITY STATEMENT**
Approved for Public Release; Distribution Unlimited

**13. SUPPLEMENTARY NOTES**

**14. ABSTRACT**

We are performing proteomic studies to identify new regulators involved in the RTK/PI3K/AKT and Hippo/YAP pathways. We discovered several new regulators in these pathways, including WWP2, which targets PTEN for degradation, and AMOTL2, which associates with YAP1 and negatively regulates YAP1 activity. In the pass funding period, we also uncovered MEMO1 as an IRS1-interacting protein and showed that MEMO1 promotes epithelial-to-mesenchymal transition via regulating IRS1/Snail. It is likely that these and other ongoing studies will reveal the roles of these interactions in breast cancer development and treatment.

**15. SUBJECT TERMS**

Tumor suppressor, Oncogene, cell proliferation, cell growth

| 16. SECURITY CLASSIFICATION OF: | | | 17. LIMITATION OF ABSTRACT | 18. NUMBER OF PAGES | 19a. NAME OF RESPONSIBLE PERSON |
|---|---|---|---|---|---|
| a. REPORT | b. ABSTRACT | c. THIS PAGE | | | USAMRMC |
| U | U | U | UU | 41 | 19b. TELEPHONE NUMBER *(include area code)* |

**Table of Contents**

## Introduction:

The goal of this proposal is to identify new components in cell survival and proliferation pathways that are known to be critical for tumor maintenance. We hope that the discovery of these new components will reveal not only the complex network involved in tumor proliferation and progression, but also new targets for cancer treatment.

## Body:

The specific Aims are:

### Specific Aim 1: Purify protein complexes involved in the PI3K/AKT and Hippo/YAP pathways.

The objective of this specific aim is to achieve a comprehensive understanding of protein-protein interaction networks involved in these two signaling pathways.

Specific Aim 1A:

Within the PI3K/AKT pathway, we initially purified PTEN-containing protein complexes. As presented in our previous annual report, we identified a HECT domain-containing E3 ubiquitin ligase WWP2 as a PTEN-associated protein. Further functional analysis revealed that WWP2 targets PTEN for polyubiquitination and degradation, indicating that WWP2 is a negative regulator of PTEN. Indeed, our subsequent studies suggest that WWP2 is required for cell proliferation, which partially depends on PTEN expression. Together these data support a hypothesis that WWP2 acts to downregulate PTEN and other unknown substrates and thus promote cell proliferation. A manuscript summarizing these data was accepted for publication (Nature Cell Biology 13:728-33, 2011; see Maddika et al., 2011).

Besides PTEN, we also purified many other protein complexes involved in the RTK/ PI3K/AKT pathways. The novel interaction we studied during this funding period is IRS1/MEMO1, which we will describe below in Specific Aim 2. In addition, we have identified several other potential interactions, which we are still confirming. These include putative associations of LKB1 with PPM1G, ERBB3/4 with PHLDA2, RPTOR with ILK2. We will first verify that these interactions occur between endogenous proteins and then further study the functional significance of these associations.

Specific Aim 1B:

For the Hippo/YAP pathway, we described in the previous annual report that AMOT and two AMOT-like proteins, AMOTL1 and AMOTL2, are YAP1-associated proteins. Our subsequent studies revealed that AMOTs are novel negative regulators of YAP1. Specifically related to breast cancer, we showed that MCF10A cells with AMOTL2 knockdown undergo epithelial-to-mesenchymal transition (EMT), a phenotype similar to that described in MCF10A cells with YAP1 overexpression (Overholtzer et al., 2006). Moreover, downregulation of YAP1 partially inhibited EMT in cells with AMOTL2 knockout, indicating that AMOTL2 regulates EMT at least in part via restraining YAP1

activity. These data were published recently (J. Biol. Chem. 286:4364-70, 2011; see Wang et al., 2011). We have conducted the purification of several other components in the Hippo/YAP pathways. In addition, we have established stable cell lines expressing SFB-tagged FARMD6, NF2, MOB1A, MOB1B and LGL2. We will purify these protein complexes shortly.

**Specific Aim 2: Investigate the functional significance of newly identified components of these signaling pathways in breast cancer development and treatment.**

1) Explore the functional significance of IRS1/MEMO interaction:

As we reported last year, MEMO1 (Mediator of ErbB2-driven cell motility 1), which was first discovered as a protein that relays extracellular signals to control cell motility (Marone et al., 2004), was also identified by us as an IRS1-associated protein. Since IRS-1 (Insulin Receptor substrate 1) and other IRS proteins are known to be involved in cancer metastasis, we decided to further explore the functional significance of this interaction.

1A) MEMO1 triggers morphology changes in monolayer and disrupts normal mammary acinar architecture in 3D matrigel culture.

As a start of this project, we first determined the function of MEMO1 in breast epithelial cells. We introduced this gene by retroviral infection into nontumorigenic human mammary epithelial cell line MCF10A. This cell line has been used extensively to examine the effects of various oncogenes on acinus formation in 3D Matrigel culture (Debnath and Brugge, 2005). To avoid any effect due to clonal selection, we performed all of the experiments with short-term cultures of pools of cells stably overexpressing MEMO1 fused with an N-terminal hemagglutinin (HA)-Flag tag (MCF10A-MEMO1). We used IRS1 and YAP as positive control oncogenes in this assay, since both of them are known to change the morphology of MCF10A cells in monolayer and 3D Matrigel culture (Dearth et al., 2006; Overholtzer et al., 2006).

Whereas control MCF10A cells grew in epithelial-type islands in monolayer cultures, cells overexpressing MEMO1, IRS1, or YAP displayed cell scattering and loss of cell–cell contacts (**Figure 1A**, upper panels). We confirmed previous reports that MCF10A-YAP1 cells form cord-like structures, indicating a highly metastatic phenotype (Overholtzer et al., 2006), and that MCF10A-IRS1 cells form larger, disrupted, irregular colonies in 3D Matrigel (Dearth et al., 2006) (**Figure 1A**, middle panels). MEMO1 expression also disrupted the normal morphogenesis of MCF10A cells in 3D Matrigel: MCF10A-MEMO1 cells failed to form spherical acinar-like structures like the control vector transfected cells did. Staining of basement membranes of acinar structures with laminin V, a marker of epithelial cell polarity, showed that control vector transfected MCF10A cells formed well-organized acinar structures with apical–basal polarity, whereas the multi-acinar structures of MCF10A-MEMO1, MCF10A-IRS1, and MCF10A-YAP cells had disrupted polarity (**Figure 1A**, bottom panels). Moreover, some MCF10A-

MEMO1 colonies had projections into Matrigel, a characteristic of invasive cells. However, instead of the expected increase in proliferation, we observed growth suppression in MCF10A-MEMO1 cells (**Figure 1A** and data not shown). This finding indicates that MEMO1 overexpression probably acts pleiotropically on various signaling pathways; a high level of MEMO1 induces cell transformation but suppresses cell growth.

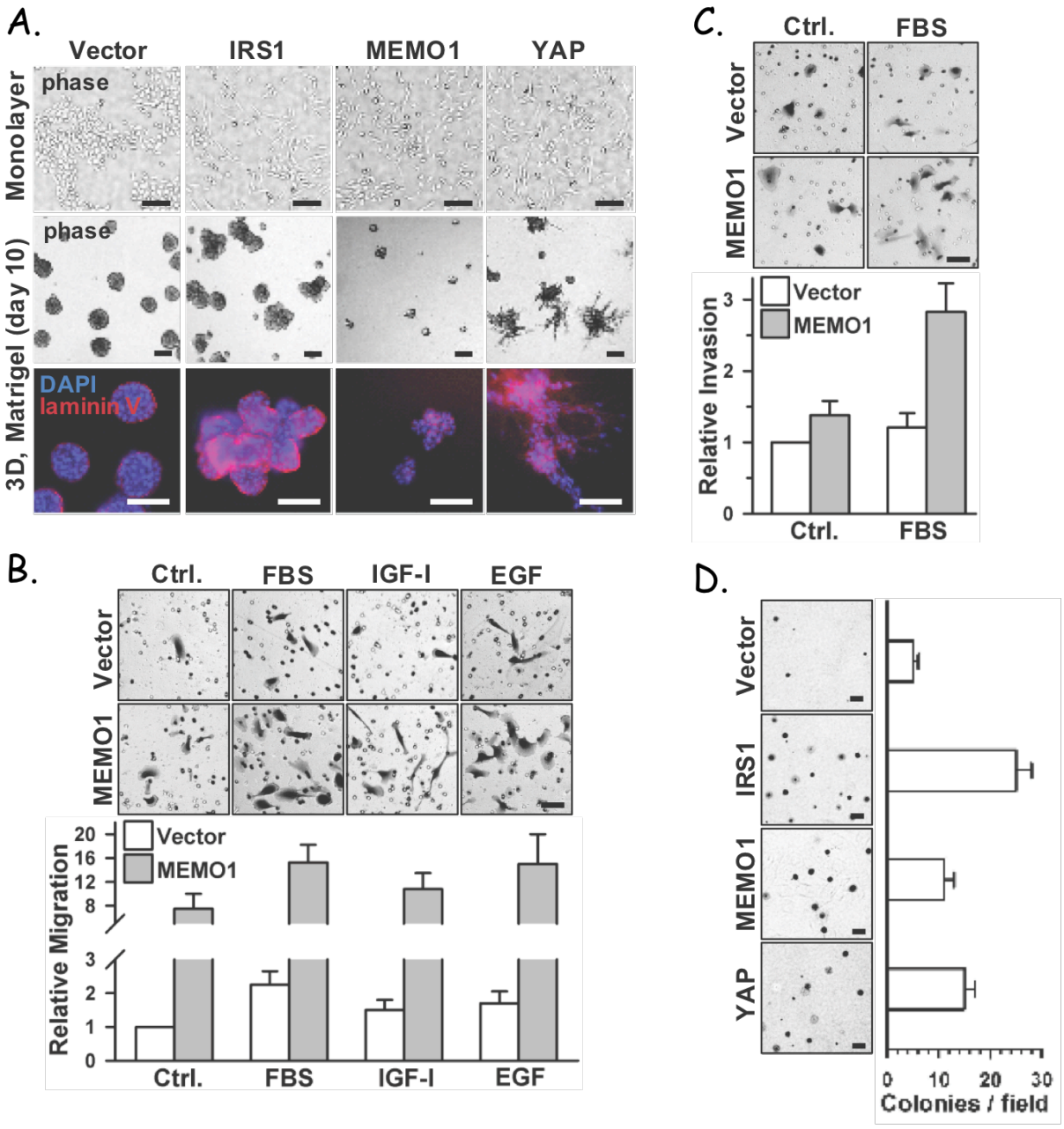


**Figure 1**. **MEMO1 disrupts mammary acinar architecture and enhances migration, invasion, and anchorage-independent growth in MCF10A Cells.**
(**A**) MCF10A cells stably transfected with empty vector or expressing HA-Flag-tagged MEMO1, IRS1, or YAP were grown in monolayer or Matrigel and examined by phase contrast and IF staining. Scale bars,

100 μm. (**B, C**) Migration (**B**) or invasion (**C**) of indicated MCF10A derivative cell lines toward FBS or growth factors were determined by transwell migration or invasion assay. Migration toward 0.5% FBS was used as a negative control. Data are the mean of two independent experiments counted in triplicate (±SD). Representative fields are shown. Scale bars, 50 μm. (**D**) Indicated MCF10A derivative cell lines were plated in soft agar and allowed to grow for 20 days. Data are the average number of colonies counted in five fields of view (±SD). Representative fields are shown. Scale bars, 100 μm.

Because MCF10A-MEMO1 cells displayed cell scattering and loss of cell–cell contacts, we hypothesized that ectopic MEMO1 expression increases cell motility. Indeed, MCF10A-MEMO1 cells displayed a remarkable capacity for migration in response to fetal bovine serum (FBS), epidermal growth factor (EGF), and IGF-I in transwell assays (**Figure 1B**). Moreover, MCF10A-MEMO1 cells showed a higher ability of invasion through Matrigel (**Figure 1C**), which agrees with previous studies indicating that MEMO1 overexpression is correlated with an invasive phenotype of cancer cells **(Hannafon et al., 2011; Kalinina et al., 2010).**

To evaluate a more stringent indicator of oncogenic transformation, we examined the effect of MEMO1 on the ability of MCF10A cells to form colonies in soft agar, a property that frequently correlates with tumorigenicity. As expected, control vector transfected MCF10A cells failed to produce large anchorage-independent colonies in soft agar. In marked contrast, MCF10A-MEMO1, MCF10A-IRS1, and MCF10A-YAP cells formed large colonies after 2 weeks in soft agar (**Figure 1D**), demonstrating that MEMO1 can induce cell transformation.

1B) MEMO1 Promotes EMT.

The highly organized, cobblestone-like morphology of MCF10A cells was replaced by spindle-like fibroblast morphology in MCF10A-MEMO1 cells, suggesting that cells overexpressing MEMO1 had undergone EMT (**Figure 2A**). Indeed, the mesenchymal markers N-cadherin and vimentin were upregulated and the epithelial markers E-cadherin, occludin, and β-catenin were all downregulated in MCF10A-MEMO1 cells, as demonstrated by immunofluorescence (IF) and immunoblotting analyses (**Figure 2C** and **2D**). MCF10A-MEMO1 cells also displayed disorganization of adherens junctions, another hallmark of EMT, as shown by E-cadherin and actin localization (**Figure 2B** and **2C**). Moreover, MEMO1 overexpression caused remodeling of focal adhesion sites in MCF10A cells (**Figure 2B**), which could explain the increased motility. Collectively, these morphological changes in monolayer and 3D Matrigel cultures and increased motility and invasion in Matrigel indicated that MEMO1 overexpression triggers EMT in MCF10A cells.

To examine whether MEMO1-induced EMT can be reversed, we generated a stable cell line, in which the *MEMO1* gene was placed under the control of doxycycline-inducible promoter. We found that doxycycline-induced MEMO1 overexpression was accompanied by EMT, but this phenotype was reversed when doxycycline was removed from growth medium (**Figure 2E** and **2F**).

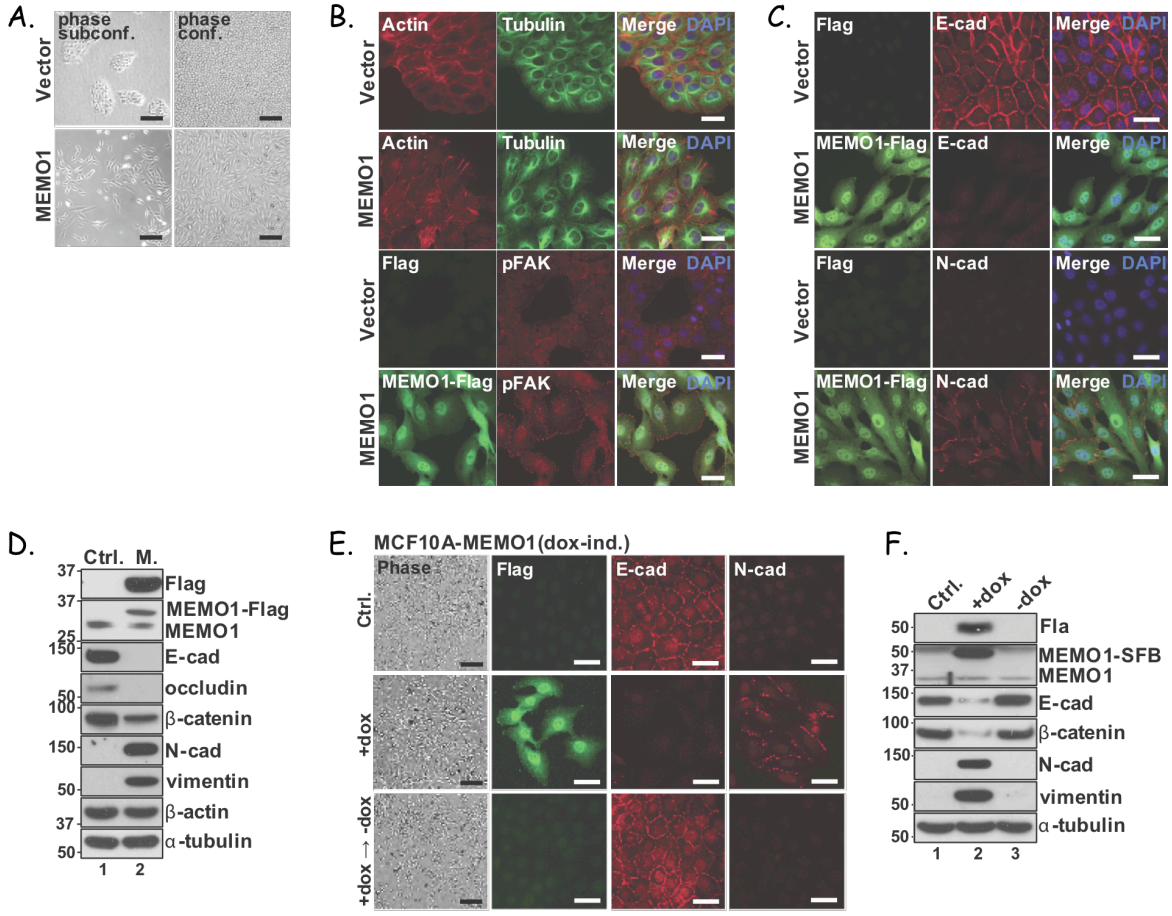


**Figure 2**. **MEMO1 induces EMT.**
(**A**) MCF10A cells stably transfected with empty vector or expressing HA-Flag-tagged MEMO1 were grown in monolayer and examined by phase contrast. Representative fields of subconfluent (subconf.) or confluent (confl.) monolayer are shown. Scale bars, 100 μm. (**B, C, D**) MCF10A cells stably transfected with empty vector or expressing HA-Flag-tagged MEMO1 were grown in monolayer and examined by IF staining (**B, C**) and WB analysis (**D**) for the expression of cytoskeletal proteins or epithelial/mesenchymal markers, as indicated. Scale bars, 20 μm. (**E, F**) MCF10A cells stably expressing SFB-tagged MEMO1 placed under the control of doxycycline-inducible (dox-ind.) promoter were grown in monolayer with or without doxycycline (1 μg/ml) in assay medium and examined by phase contrast (**E**; scale bars, 100 μm), IF staining (**E**; scale bars, 20 μm) and WB analysis (**F**).

## 1C) MEMO1 Triggers EMT in an IRS1/Snail1-Dependent Manner.

Various stimuli within the tumor microenvironment promote EMT of cancer cells (Kalluri and Weinberg, 2009)**.** To gain insight into the mechanism by which MEMO1 triggers EMT, we examined whether MEMO1 expression could activate signaling through either ERK or Akt, two major signaling pathways that can contribute to EMT in MCF10A cells. We found that the PI3K/Akt pathway, but not the MEK/ERK pathway, was strongly activated even under basal conditions, without stimulation by growth factors (**Figure 3A**). Moreover, we observed a mild inhibition of the MEK/ERK pathway. Although MEMO1 was originally identified as an adaptor of HER2 (Marone et al., 2004)**,** here we

observed that PI3K/Akt pathway was activated after stimulation of cells by IGF-I, but not by EGF, indicating the dependence of MEMO1-induced cell signaling activation on IGF-IR/IRSs (**Figure 3A**). As expected, knockdown of MEMO1 by shRNAs had the opposite effect on PI3K/Akt signaling, i.e., a mild suppression of Akt (**Figure 3B**).

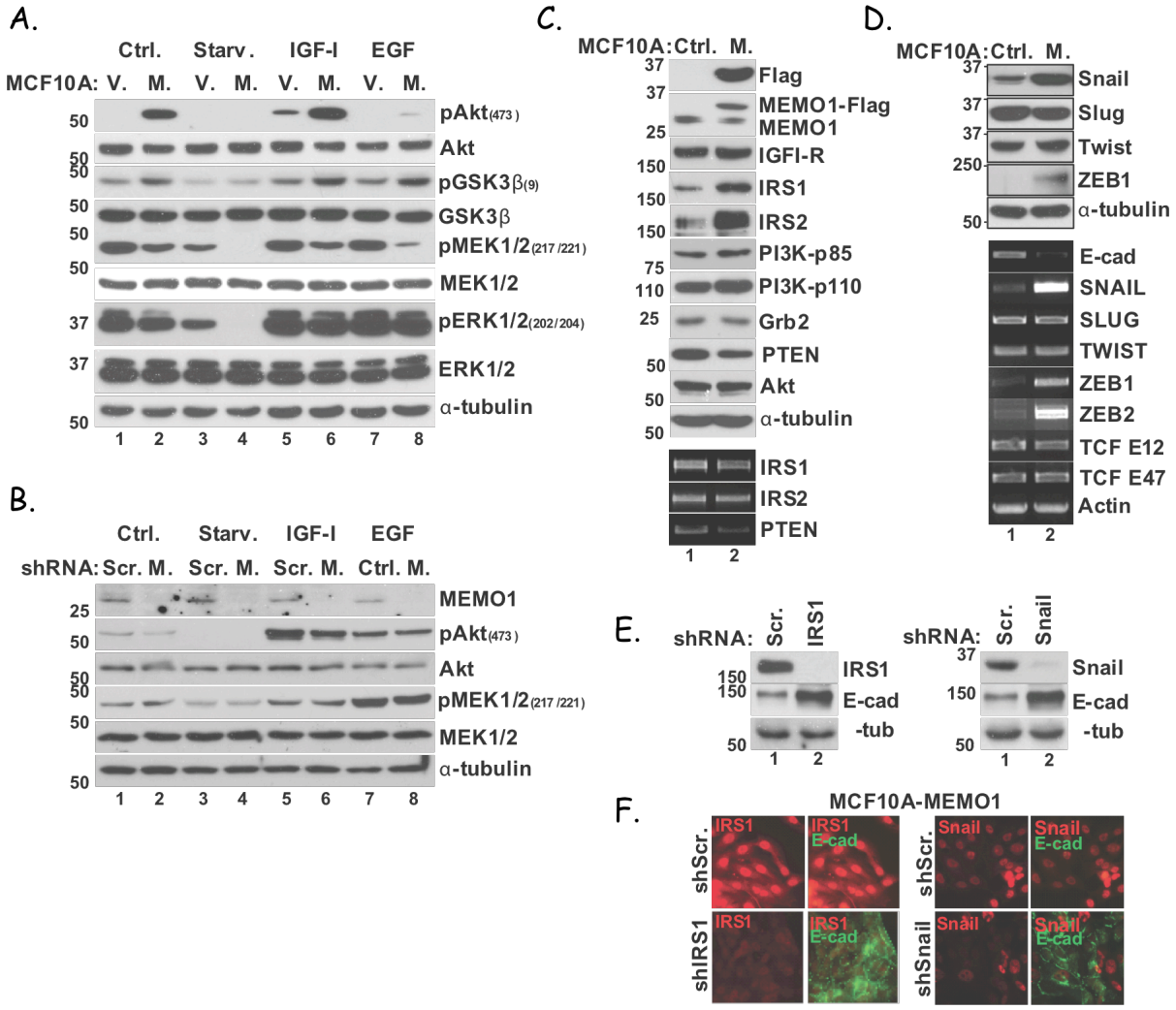


**Figure 3**. **IRS1 and Snail1 are both required for MEMO1-induced EMT.**
(**A**) MCF10A cells stably transfected with empty vector (V.) or expressing HA-Flag-tagged MEMO1 (M.) were grown in monolayer in normal (Ctrl.) or low-serum (Starv.) medium or were stimulated by growth factors after serum starvation and then examined for signaling molecules by WB analysis using antibodies as indicated. (**B**) MCF10A cells were transiently infected with viruses expressing scrambled (Scr.) or MEMO1 (M.) shRNAs and examined as that described in (**A**). (**C, D**) MCF10A cells, as in (**A**), were examined for levels of signaling molecules and transcription factors by WB analysis and RT-PCR. (**E, F**) MCF10A cells stably expressing HA-Flag-tagged MEMO1 were transiently infected with viruses overexpressing scrambled (Scr.), IRS1, or Snail shRNAs and were examined by WB analysis (**E**) and IF staining (**F**) using antibodies as indicated. Scale bars, 20 μm.

A major driving force of EMT is the repression of epithelial cell–cell junction protein E-cadherin. About a dozen transcriptional repressors (e.g., Snail, Slug, Twist, ZEB1/2, and TCF E12/E47) can suppress E-cadherin expression in the cell (Kalluri and Weinberg,

2009; Sabbah et al., 2008). Reverse transcriptase PCR (RT-PCR) analysis showed that MEMO1 overexpression results in overexpression of Snail and ZEB1/2 mRNAs in MCF10A cells (**Figure 3D**), suggesting a possible mechanism for the effect of MEMO1 on EMT.

The current model of how the activation of the IGF-IR/IRSs signaling pathway triggers EMT is following: IGF-I/IGF-II binding to the extracellular α-subunits of IGF-IR results in activation of the intrinsic tyrosine kinase within the intracellular part of the IGF-IR β-subunit, which induces autophosphorylation and leads to recruitment and tyrosine (Tyr) phosphorylation of IRS docking proteins (Werner and Le Roith, 2000). Concomitant binding and phosphorylation of the p85 regulatory subunit of PI3K, causes PI3K activation, and, via PI(3,4,5)P3, leads to stimulation of PI-dependent kinase (PDK) and activation of Akt (Butler et al., 1998; Cantley, 2002; LeRoith and Roberts, 2003). Activation of Akt leads to the suppression of GSK3β (Cross et al., 1995), which is known to phosphorylate and destabilize Snail protein (Yook et al., 2005; Zhou et al., 2004). NF-κB is activated in an Akt-dependent manner (Bachelder et al., 2005) and activates transcription of Snail and ZEB1/2 mRNAs (Bachelder et al., 2005; Chua et al., 2007; Julien et al., 2007; Wu et al., 2009). In addition, Snail may also be involved in the activation of *ZEB1/2* gene expression (Guaita et al., 2002). An increase in Snail and ZEB1/2 protein expression leads to the suppression of E-cadherin and thereby triggers EMT (Comijn et al., 2001; Escriva et al., 2008; Grooteclaes and Frisch, 2000). Moreover, Snail suppresses expression of *PTEN* gene (Batlle et al., 2000), which is an Akt suppressor (Maehama and Dixon, 1998).

We found that MEMO1-induced EMT was consistent with the proposed mechanism of IGF-IR/IRSs/Akt/Snail-dependent EMT. Akt was activated in MEMO1-overexpressing cells (**Figure 3A**), which resulted in the accumulation of Snail and ZEB1 proteins (**Figure 3D**). Moreover, the PTEN level was markedly decreased, whereas the IRS1 level was increased (**Figure 3C**). The decrease in PTEN level could be explained by the suppression of its transcription by Snail, whereas the increase in IRS1 level was probably due to protein stabilization (**Figure 3C**). More directly, we showed that knockdown of IRS1 or Snail1 in MCF10A-MEMO1 cells de-repressed E-cadherin synthesis (**Figure 3E and 3F**). Collectively, these data indicate that MEMO1 triggers EMT in MCF10A cells in an IRS1/Snail-dependent manner.

2) <u>AMOTL2 negatively regulates AKT activity.</u>

We reported earlier that knockdown of AMOTL2 led to epithelial-mesenchymal transition (Wang et al., 2011). We also detected enhanced AKT activation in MCF10A cells with AMOTL2 depletion (Wang et al., 2011) . Indeed, phosphorylation of AKT on both Thr308 and Ser473 sites increased in cells with AMOTL2 knockdown (**Figure 4A**). This increase of AKT phosphorylation was not observed in cells transfected with control shRNA or cells with AMOTL1 knockdown (**Figure 4A**). Moreover, phosphorylation of GSK3β, which is one of the AKT downstream effectors, also increased in AMOTL2 knockdown cells, while the levels of several upstream regulators of AKT, including PTEN and PI3K, remained the same in these cells (**Figure 4A**). On the other hand, the

phosphorylation of AKT and its downstream effecter GSK3β was inhibited in cells with AMOTL2 overexpression (**Figure 4B).** Together, these data suggest that AMOTL2 negatively regulates AKT activity.

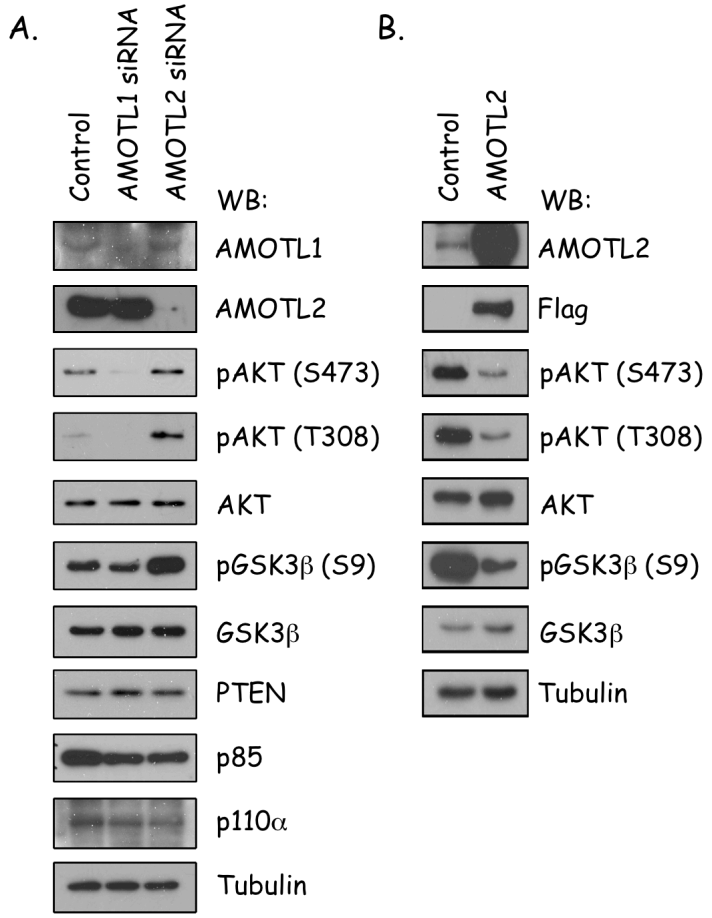


**Figure 4. AMOTL2 negatively regulates AKT signaling in MCF10A cells.**
(**A**) Knockdown AMOTL2 in MCF10A cells increased AKT phosphorylation. (**B**) Overexpressing AMOTL2 inhibited AKT phosphorylation. Western blotting was conducted with indicated antibodies.

Although AKT was activated in AMOTL2 knockdown cells, we did not observe any change of PI3K and PTEN in these cells (**Figure 4A**), which raised the possibility that AMOTL2 may directly regulate AKT. As a matter of fact, we found that AMOTL2 associated with AKT1, but not with PTEN (**Figure 5A**). Bacterially expressed and purified GST-AKT1 was able to pull-down SFB-AMOT2 from cell extract (**Figure 5B**). Moreover, AMOTL2 binds to both inactive AKT1 (K179M) and constitutively activated AKT1 (Myr tag fused AKT1) in the cell (**Figure 5C**). To determine the domains of AMOTL2 that interact with AKT1, we generated SFB tag fused AMOTL2 truncations containing N-terminal glutamine rich domain (GRD, amino acids 1~306), middle region coiled-coil domain (Coiled-coil, amino acids 307~580) and C-terminal domain (CT, amino acids 581~780) (**Figure 5D**). We found AKT1 can associate with GRD and CT domains, but not Coiled-coil domain of AMOTL2 (**Figure 5E**). These data indicate both N-terminus and C-terminus of AMOTL2 are involved in its binding to AKT1.

To identify the domains of AKT1 required for AMOTL2 binding, GFP tag fused PH domain (PH, amino acids 1~148), kinase domain (Kinase, amino acids 149~407) and C-terminal domain (CT, amino acids 408~480) of AKT1 were co-transfected with AMOTL2 in 293T cells (**Figure 5D**). AMOTL2 has very strong interactions with AKT1 PH and C-terminal domains compared with full length AKT1. Compared with the PH and C-terminal domains, we noticed full-length AKT1 had weaker interaction with AMOTL2, which was probably due to the protein structure protection. Besides, we detected very

weak interaction between AMOTL2 and AKT1 kinase domain (**Figure 5F**). These results showed multiple regions of AKT1 contribute to its association with AMOTL2.

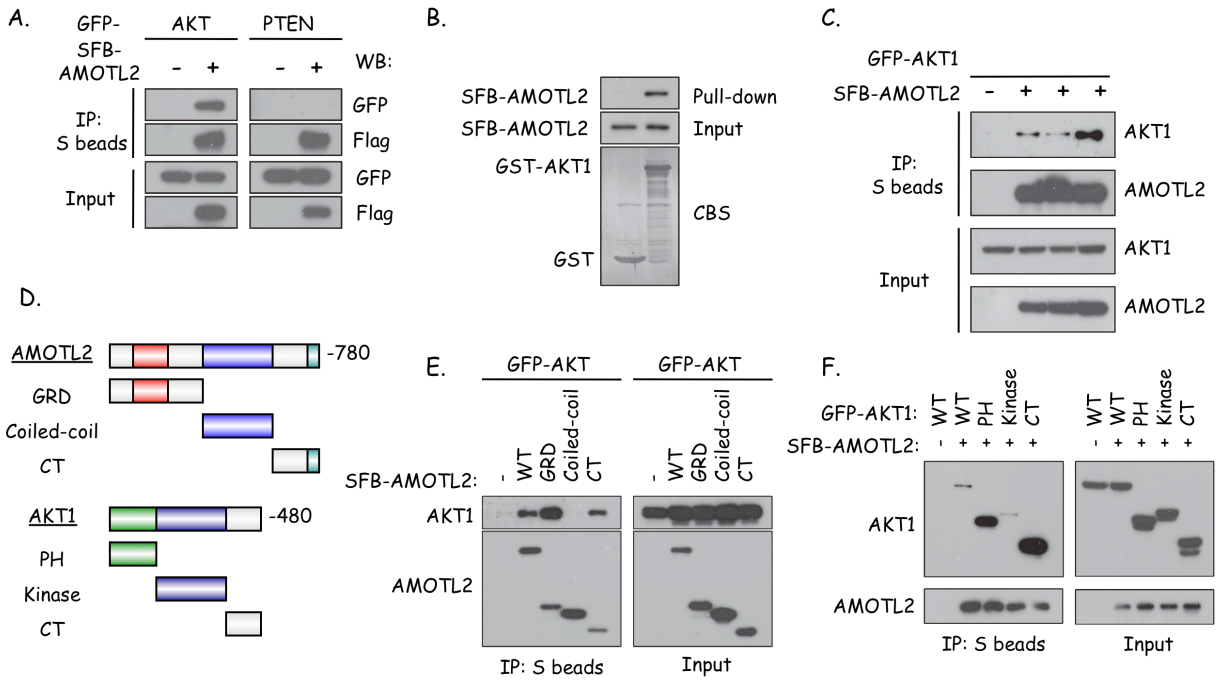


**Figure 5. AMOTL2 associates with AKT.**
(**A**) AMOTL2 specifically interacts with AKT, but not with PTEN in PI3K-AKT. Constructs encoding SFB tagged AMOTL2 was co-tranfected with constructs encoding GFP tagged AKT1 or PTEN into 293T cells. S beads were used to precipitate AMOTL2 and co-precipitated GFP-AKT1 or GFP-PTEN was analyzed by immunoblotting as indicated. (**B**) AMOTL2 interacts with AKT. Sepharose beads containing Glutathione-S-transferase (GST) or GST-AKT1 fusion protein were incubated with cell lysates containing exogenously expressed SFB-AMOTL2. Associated AMOTL2 protein was detected by Western blotting using anti-FLAG antibody. The amount of GST and GST-AKT1 used in this experiment was shown by Coomassie blue staining (CBS). (**C**) AMOTL2 interacts with both inactive and active forms of AKT1. Plasmids encoding SFB-tagged AMOTL2 was co-transfected with plasmids encoding GFP tagged wild-type AKT1, inactive AKT1 (K179M) or constitutively active form of AKT1 (myristoylated-AKT1). S beads were used to precipitate associated proteins and Western blotting was conducted using anti-GFP or anti-FLAG antibodies. (**D**) Schematic diagrams of the domain structures for human AMOTL2 and AKT1. (**E, F**) Constructs encoding SFB tagged full-length or truncated AMOT2 proteins were co-transfected with plasmids encoding GFP-AKT1 (**E**). Alternatively, plasmids encoding SFB-AMOTL2 were co-transfected with plasmids encoding eGFP fused full-length or truncated form of AKT1 (**F**). Precipitation and Western blotting were performed as indicated.

We observed AMOTL2 can suppress AKT activation through down-regulating AKT phosphorylation on both Ser473 and Thr308 sites (**Figure 4**). Since AMOTL2 is a cytoplasmic protein, which can bind to both inactive and active forms of AKT1 (**Figure 5C**), we hypothesized that AMOTL2 might impair the ability of AKT to translocate from cytoplasm to the plasma membrane, thereby inhibiting AKT phosphorylation and activation. To test this hypothesis, cells were transfected with constructs expressing GFP-tagged AKT1 alone or together with those expressing SFB-tagged AMOTL2. After serum starvation, cells were treated with 20% FBS for 20 minutes and followed by immunofluoresent staining. In serum starved cells only expressing GFP-AKT1, AKT1

localized in both nuclear and cytoplasm. However, following serum stimulation, we observed the translocation of GFP-AKT1 to plasma membrane (**Figure 6A**). In contrast, when co-expressed with AMOTL2, even in serum-starved cells, AKT1 was highly concentrated in the cytoplasm, where it co-localized with AMOTL2. Following serum stimulation, we also failed to detect plasma membrane translocation of AKT1 (**Figure 6A**). To confirm that AMOTL2 can inhibit AKT translocation, we also expressed GFP-tagged fused myr-AKT1, which associates with plasma membrane and constitutive active, alone or with AMOTL2. Indeed, myr-AKT1 can localize at plasma membrane (**Figure 6B**). However, when co-expressed with AMOTL2, myr-AKT1 was sequestered in the cytoplasm and showed extensive co-localization with AMOTL2 (**Figure 6B**). These data indicate that AMOTL2 can regulate AKT translocation and thus negatively regulate AKT activation in the cell.

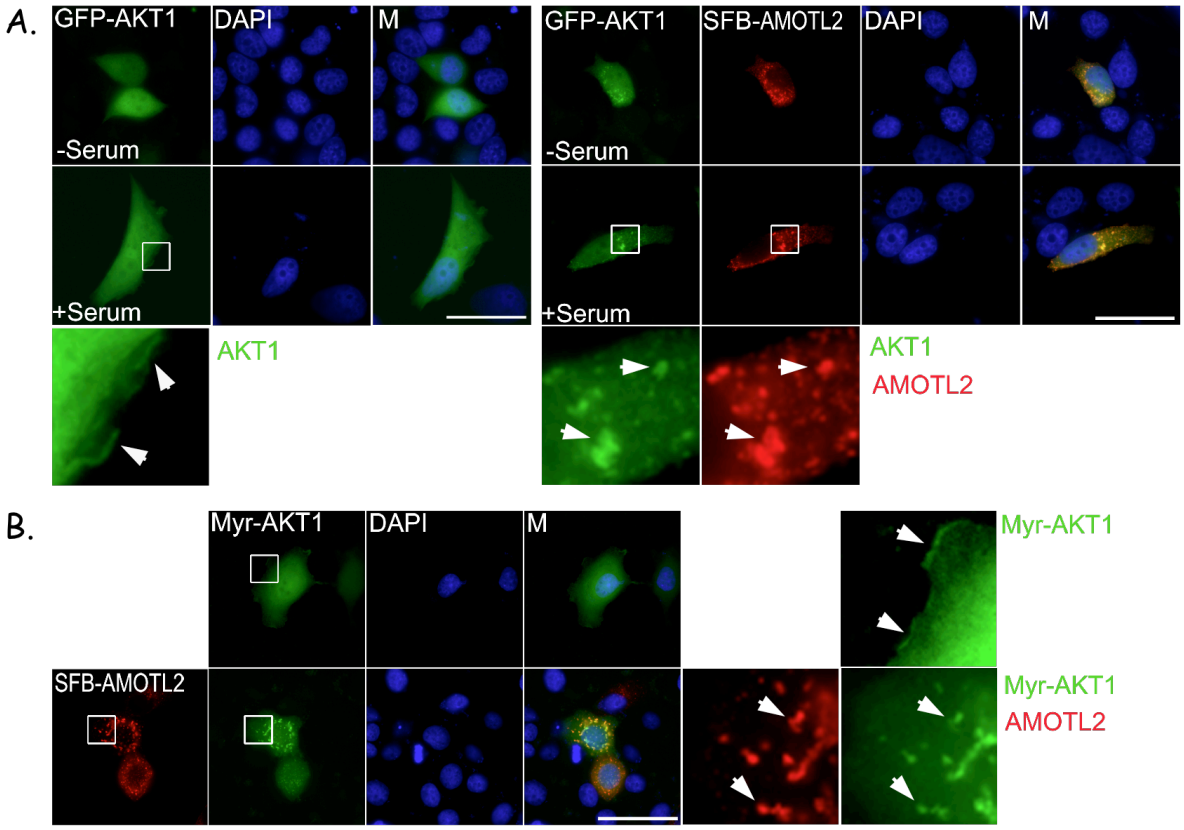


**Figure 6. AMOTL2 inhibits AKT translocation to plasma membrane.** (**A**) AMOTL2 blocks serum stimulated plasma membrane translocation of AKT. HeLa cells were transfected with plasmids encoding GFP-AKT with or without plasmids encoding SFB-AMOTL2. Immunofluoresent staining was performed to detect the GFP-AKT localization before and after serum stimulation. (**B**) AMOTL2 sequesters myristoylated AKT in cytosol. HeLa cells were transfected with plasmids encoding GFP-myr-AKT1 with or without plasmids encoding SFB-AMOTL2. Immunofluoresent staining was performed as indicated. Scale bar=40mm.

Based on the observation that AMOTL2 could suppress AKT activation and AKT-dependent signaling pathway, we wondered whether AMOTL2 might adversely affect cell proliferation. Indeed, AMOTL2 knockdown cells exhibited increased BrdU

incorporation (**Figure 7A**). AMOTL2 knockdown cells also grew faster than control knockdown cells (**Figure 7B**).

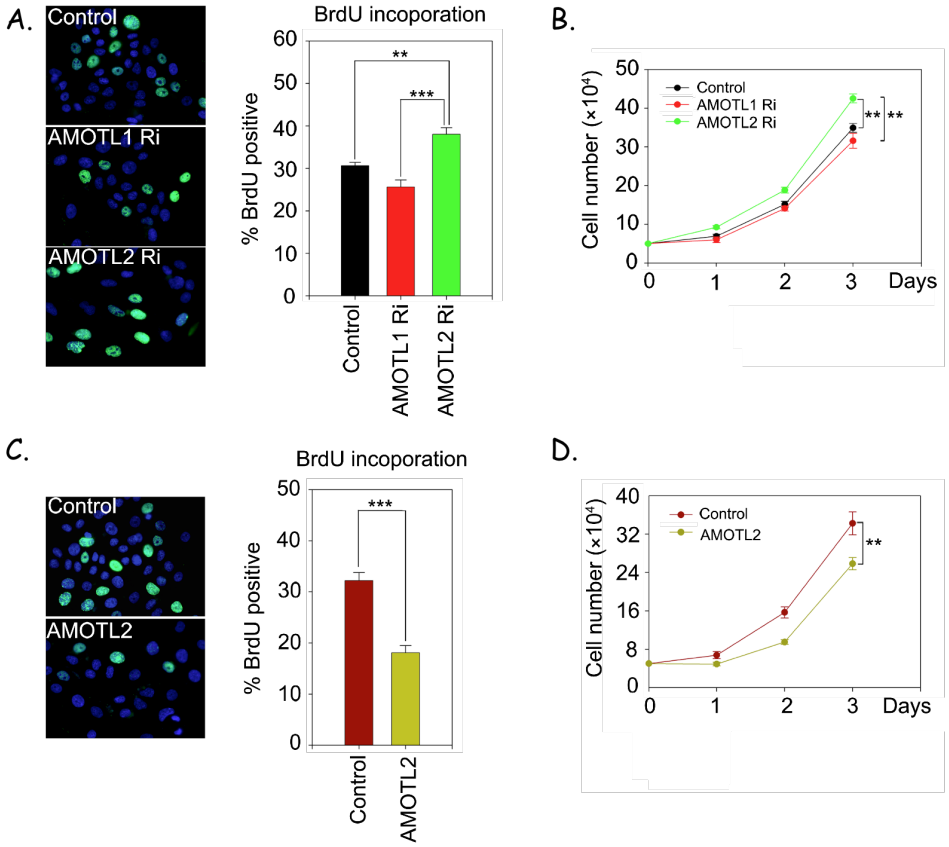


**Figure 7. AMOTL2 negatively regulates cell proliferation.**
(**A**) Control knockdown, AMOTL1 knockdown or AMOTL2 knockdown MCF10A cells were incubated with 10 μM BrdU for 2 hours. Cells were fixed and subjected to immunofluoresent staining using Alexa Fluor-488 anti-BrdU antibody. The percentages of BrdU positive cells were shown (n=3, ** means p<0.01, *** means p<0.001, mean±SEM). (**B**) Cell proliferation was increased in AMOTL2 knockdown cells (n=3, **means p<0.01, mean±SEM). (**C**) Control cells or cells with AMOTL2 overexpression were incubated with BrdU and percentages of BrdU positive cells were determined (n=3, *** means p<0.001, mean±SEM). (**D**) Cell proliferation was reduced in cells with AMOTL2 overexpression (n=3, **means p<0.01, mean±SEM).

Conversely, in MCF10A cells with AMOTL2 overexpression, the BrdU incorporation was reduced compared with vector control cells (**Figure 7C**). Cells with AMOTL2 overexpression also showed reduced proliferation when compared with control cells transfected with empty vector (**Figure 7D**). These data suggest that AMOTL2 negatively regulate cell proliferation *in vivo*.

In the study presented above, we showed that AMOTL2 negatively regulates AKT activation, which is likely mediated by the ability of AMOTL2 to inhibit AKT translocation to plasma membrane and thus sequester AKT as inactive kinase in the intracellular fractions. Exactly how AMOTL2 is regulated to associate with AKT and regulate AKT translocation and activation is an important question that needs to be addressed in future studies. Nevertheless, together with our previous study of AMOTL2/YAP1 association (Wang et al., 2011), it becomes clear that AMOL2 is an important regulator of cell growth and proliferation. Further studies of AMOTL2 in breast cancer development will likely yield new insights into the complex regulation of tumor growth.

3) <u>Explore YAP1/PTPN14 association.</u>

When we isolated YAP1-containing protein complexes from MCF10A cells, we not only confirmed the interactions of YAP1 with AMOTL1/L2, TEAD1 and 14-3-3 (**Figure 8A**), but also identified two new YAP1-associated proteins, PTPN14 and PTPN21 (**Figure 8A**). PTPN14 and PTPN21 are two related protein tyrosine phosphatases. Both of them contain FERM domain at N-termini and phosphatase domain at C-termini (**Figure 8B**). Moreover, both of them contain PY motifs, suggesting that they may interact with WW domains of YAP1 via these PY motifs.

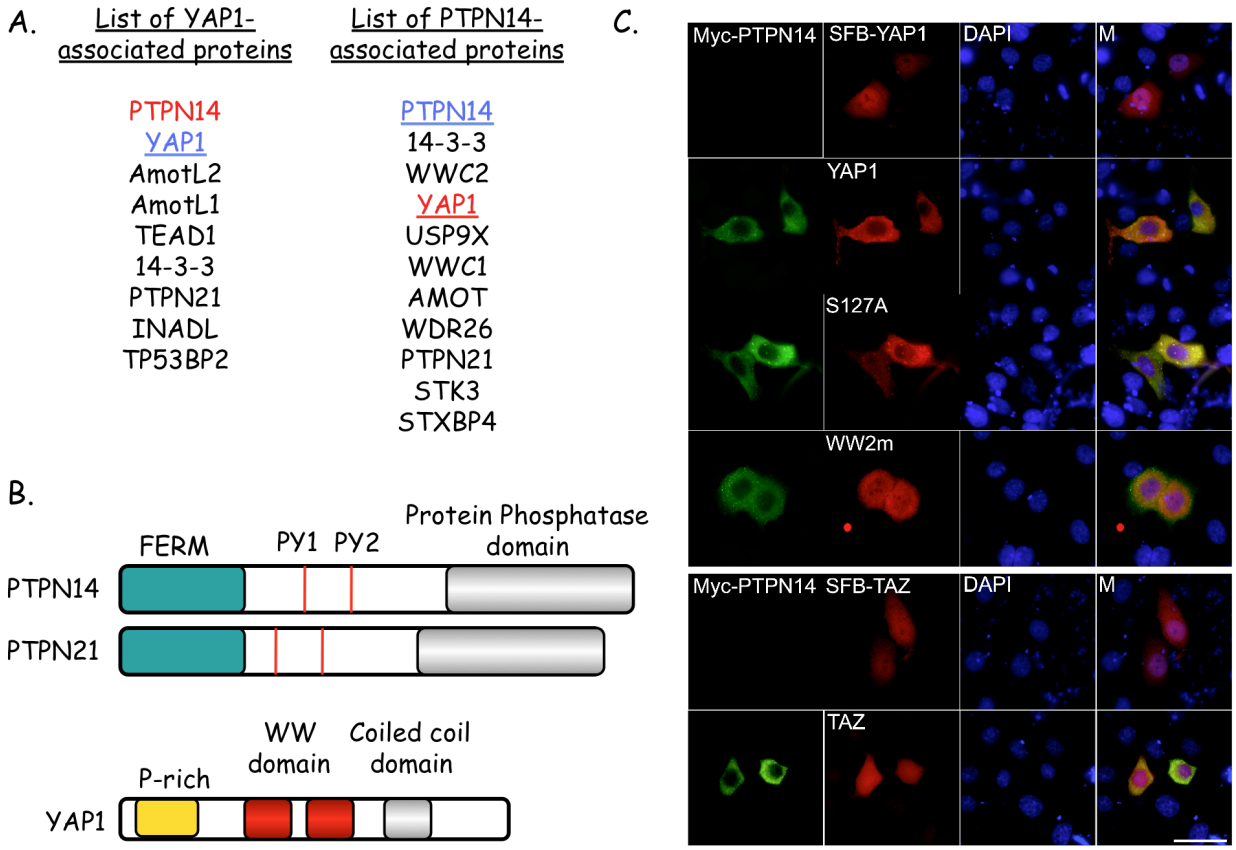


**Figure 8. YAP1 associates with PTPN14.** (**A**) Tandem affinity purification followed by mass spectrometry analysis revealed an interaction between PTPN14 and YPA1. (**B**) Domain structures of PTPN14/21 and YAP1 are indicated. (**C**) PTPN14 sequesters YAP1 but not TAZ in cytosol. HeLa cells were transfected with plasmids encoding Myc-tagged PTPN14 with plasmids encoding SFB-tagged wild-type or mutant YAP1 (or TAZ). Immunofluoresent staining was performed using ant-Myc or anti-Flag antibodies.

We performed reverse purification using tagged PTPN14 and verified that YAP1 is a major PTPN14-associated protein in MCF10A cells (**Figure 8A**). We also confirm that the interaction between PTPN14 and YAP1 is mediated by their respective PY motifs and WW domains (data not shown). More over, we showed that PTPN14 interacts with YAP1 but not its close homolog TAZ (data not shown). In addition, PTPN14 overexpression leads to the retention of YAP1, but not TAZ, in cytosol (**Figure 8C**). Together, these data indicated a specific interaction between YAP1 and PTPN14. We are currently investigating the functional significance of this interaction in breast cancer development and progression.

## Key Research Accomplishments:

- MEMO1 promotes EMT in an IRS1/Snail1-dependent manner.

- AMOTL2 negatively regulates AKT activity via sequestering AKT in cytosol.

## Reportable Outcomes:

Manuscripts:

Maddika S, Kavela S, Rani N, Palicharla VR, Pokorny JL, Sarkaria JN, **Chen J.** WWP2 is an E3 ubiquitin ligase for PTEN. Nat Cell Biol. 2011 Jun;13(6):728-33.

Wang W, Huang J, **Chen J.** Angiomotin-like proteins associate with and negatively regulate YAP1. J Biol Chem. 2011 Feb 11;286(6):4364-70.

Abstracts and Presentations: None

Patents and Licenses: None

Development of Cell lines, tissue or serum repositories: None

Animal models and databases: None

Funding applied for: None

Employment or Research opportunities applied for: None

## Conclusions:

The projects are progressing as planned. We have already identified several novel regulators involved in RTK/AKT/mTOR and Hippo/YAP pathways. The one we are particularly excited about is the involvement of IRS1/MEMO1 in EMT and their abilities to transform non-tumorigenic MCF10A cells. We speculate that IRS1/MEMO1 may be involved in breast cancer development and metastasis. We will continue to study this and several other novel interactions and explore whether any of these interactions are deregulated and/or participate in breast cancer development.

## References:

Bachelder, R.E., Yoon, S.O., Franci, C., de Herreros, A.G., and Mercurio, A.M. (2005). Glycogen synthase kinase-3 is an endogenous inhibitor of Snail transcription: implications for the epithelial-mesenchymal transition. J Cell Biol *168*, 29-33.

Batlle, E., Sancho, E., Franci, C., Dominguez, D., Monfar, M., Baulida, J., and Garcia De Herreros, A. (2000). The transcription factor snail is a repressor of E-cadherin gene expression in epithelial tumour cells. Nat Cell Biol *2*, 84-89.

Butler, A.A., Yakar, S., Gewolb, I.H., Karas, M., Okubo, Y., and LeRoith, D. (1998). Insulin-like growth factor-I receptor signal transduction: at the interface between physiology and cell biology. Comp Biochem Physiol B Biochem Mol Biol *121*, 19-26.

Cantley, L.C. (2002). The phosphoinositide 3-kinase pathway. Science *296*, 1655-1657.

Chua, H.L., Bhat-Nakshatri, P., Clare, S.E., Morimiya, A., Badve, S., and Nakshatri, H. (2007). NF-kappaB represses E-cadherin expression and enhances epithelial to mesenchymal transition of mammary epithelial cells: potential involvement of ZEB-1 and ZEB-2. Oncogene *26*, 711-724.

Comijn, J., Berx, G., Vermassen, P., Verschueren, K., van Grunsven, L., Bruyneel, E., Mareel, M., Huylebroeck, D., and van Roy, F. (2001). The two-handed E box binding zinc finger protein SIP1 downregulates E-cadherin and induces invasion. Mol Cell *7*, 1267-1278.

Cross, D.A., Alessi, D.R., Cohen, P., Andjelkovich, M., and Hemmings, B.A. (1995). Inhibition of glycogen synthase kinase-3 by insulin mediated by protein kinase B. Nature *378*, 785-789.

Dearth, R.K., Cui, X., Kim, H.J., Kuiatse, I., Lawrence, N.A., Zhang, X., Divisova, J., Britton, O.L., Mohsin, S., Allred, D.C.*, et al.* (2006). Mammary tumorigenesis and metastasis caused by overexpression of insulin receptor substrate 1 (IRS-1) or IRS-2. Mol Cell Biol *26*, 9302-9314.

Debnath, J., and Brugge, J.S. (2005). Modelling glandular epithelial cancers in three-dimensional cultures. Nat Rev Cancer *5*, 675-688.

Escriva, M., Peiro, S., Herranz, N., Villagrasa, P., Dave, N., Montserrat-Sentis, B., Murray, S.A., Franci, C., Gridley, T., Virtanen, I.*, et al.* (2008). Repression of PTEN phosphatase by Snail1 transcriptional factor during gamma radiation-induced apoptosis. Mol Cell Biol *28*, 1528-1540.

Grooteclaes, M.L., and Frisch, S.M. (2000). Evidence for a function of CtBP in epithelial gene regulation and anoikis. Oncogene *19*, 3823-3828.

Guaita, S., Puig, I., Franci, C., Garrido, M., Dominguez, D., Batlle, E., Sancho, E., Dedhar, S., De Herreros, A.G., and Baulida, J. (2002). Snail induction of epithelial to mesenchymal transition in tumor cells is accompanied by MUC1 repression and ZEB1 expression. J Biol Chem *277*, 39209-39216.

Hannafon, B.N., Sebastiani, P., de Las Morenas, A., Lu, J., and Rosenberg, C.L. (2011). Expression of microRNA and their gene targets are dysregulated in preinvasive breast cancer. Breast Cancer Res *13*, R24.

Julien, S., Puig, I., Caretti, E., Bonaventure, J., Nelles, L., van Roy, F., Dargemont, C., de Herreros, A.G., Bellacosa, A., and Larue, L. (2007). Activation of NF-kappaB by Akt upregulates Snail expression and induces epithelium mesenchyme transition. Oncogene *26*, 7445-7456.

Kalinina, T., Gungor, C., Thieltges, S., Moller-Krull, M., Penas, E.M., Wicklein, D., Streichert, T., Schumacher, U., Kalinin, V., Simon, R.*, et al.* (2010). Establishment and characterization of a new human pancreatic adenocarcinoma cell line with high metastatic potential to the lung. BMC Cancer *10*, 295.

Kalluri, R., and Weinberg, R.A. (2009). The basics of epithelial-mesenchymal transition. J Clin Invest *119*, 1420-1428.

LeRoith, D., and Roberts, C.T., Jr. (2003). The insulin-like growth factor system and cancer. Cancer Lett *195*, 127-137.

Maddika, S., Kavela, S., Rani, N., Palicharla, V.R., Pokorny, J.L., Sarkaria, J.N., and Chen, J. (2011) WWP2 is an E3 ubiquitin ligase for PTEN. Nat Cell Biol *13*, 728-733.

Maehama, T., and Dixon, J.E. (1998). The tumor suppressor, PTEN/MMAC1, dephosphorylates the lipid second messenger, phosphatidylinositol 3,4,5-trisphosphate. J Biol Chem *273*, 13375-13378.

Marone, R., Hess, D., Dankort, D., Muller, W.J., Hynes, N.E., and Badache, A. (2004). Memo mediates ErbB2-driven cell motility. Nat Cell Biol *6*, 515-522.

Overholtzer, M., Zhang, J., Smolen, G.A., Muir, B., Li, W., Sgroi, D.C., Deng, C.X., Brugge, J.S., and Haber, D.A. (2006). Transforming properties of YAP, a candidate oncogene on the chromosome 11q22 amplicon. Proc Natl Acad Sci U S A *103*, 12405-12410.

Sabbah, M., Emami, S., Redeuilh, G., Julien, S., Prevost, G., Zimber, A., Ouelaa, R., Bracke, M., De Wever, O., and Gespach, C. (2008). Molecular signature and therapeutic perspective of the epithelial-to-mesenchymal transitions in epithelial cancers. Drug Resist Updat *11*, 123-151.

Wang, W., Huang, J., and Chen, J. (2011). Angiomotin-like proteins associate with and negatively regulate YAP1. The Journal of biological chemistry *286*, 4364-4370.

Werner, H., and Le Roith, D. (2000). New concepts in regulation and function of the insulin-like growth factors: implications for understanding normal growth and neoplasia. Cell Mol Life Sci *57*, 932-942.

Wu, Y., Deng, J., Rychahou, P.G., Qiu, S., Evers, B.M., and Zhou, B.P. (2009). Stabilization of snail by NF-kappaB is required for inflammation-induced cell migration and invasion. Cancer Cell *15*, 416-428.

Yook, J.I., Li, X.Y., Ota, I., Fearon, E.R., and Weiss, S.J. (2005). Wnt-dependent regulation of the E-cadherin repressor snail. J Biol Chem *280*, 11740-11748.

Zhou, B.P., Deng, J., Xia, W., Xu, J., Li, Y.M., Gunduz, M., and Hung, M.C. (2004). Dual regulation of Snail by GSK-3beta-mediated phosphorylation in control of epithelial-mesenchymal transition. Nat Cell Biol *6*, 931-940.

**Appendices:**

Manuscript 1: Maddika S, Kavela S, Rani N, Palicharla VR, Pokorny JL, Sarkaria JN, Chen J. WWP2 is an E3 ubiquitin ligase for PTEN. Nat Cell Biol. 2011 Jun;13(6):728-33.

Manuscript 2: Wang W, Huang J, Chen J. Angiomotin-like proteins associate with and negatively regulate YAP1. J Biol Chem. 2011 Feb 11;286(6):4364-70.

nature cell biology

# WWP2 is an E3 ubiquitin ligase for PTEN

Subbareddy Maddika[1,4], Sridhar Kavela[1], Neelam Rani[1], Vivek Reddy Palicharla[1], Jenny L. Pokorny[2], Jann N. Sarkaria[2] and Junjie Chen[3,4]

**PTEN, a lipid phosphatase, is one of the most frequently mutated tumour suppressors in human cancer. Several recent studies have highlighted the importance of ubiquitylation in regulating PTEN tumour-suppressor function, but the enzymatic machinery required for PTEN ubiquitylation is not clear. In this study, by using a tandem affinity-purification approach, we have identified WWP2 (also known as atrophin-1-interacting protein 2, AIP-2) as a PTEN-interacting protein. WWP2 is an E3 ubiquitin ligase that belongs to the NEDD4-like protein family, which is involved in regulating transcription, embryonic stem-cell fate, cellular transport and T-cell activation processes. We show that WWP2 physically interacts with PTEN and mediates its degradation through a ubiquitylation-dependent pathway. Functionally, we show that WWP2 controls cellular apoptosis and is required for tumorigenicity of cells. Collectively, our results reveal a functional E3 ubiquitin ligase for PTEN that plays a vital role in tumour-cell survival.**

PTEN (phosphatase and tensin homologue deleted on chromosome 10) is a well-defined tumour suppressor that plays a critical role in cell survival and cell death[1–3]. *PTEN* is either mutated or deleted with high frequency in various types of human cancer to promote tumorigenesis[3–7]. Homozygous deletion of *Pten* in mice leads to embryonic lethality, whereas *Pten*-heterozygous mice develop spontaneous tumours in multiple tissues[8–10]. The importance of PTEN as a tumour suppressor was also supported by the occurrence of *PTEN* germline mutations in a group of autosomal dominant syndromes such as Cowden syndrome, Bannayan–Riley–Ruvalcaba syndrome and Lhermitte–Duclos diseases, which are characterized by hamartomatous overgrowth of various tissues and predisposition to the development of breast, thyroid and endometrial cancers[11–13].

Functionally, PTEN is a lipid phosphatase[14,15], which antagonizes the cellular phosphatidylinositol 3-kinase (PI3K) signalling pathway. Activation of membrane receptor tyrosine kinases by external growth factors initiates the PI3K signalling pathway[16–18], which leads to downstream activation of lipid kinase PI3K. Once activated, PI3K phosphorylates phosphatidylinositol 4,5-bisphosphate (PtdIns(4,5)$P_2$) and converts it to phosphatidylinositol 3,4,5-triphosphate (PtdIns(3,4,5)$P_3$). In turn, PtdIns(3,4,5)$P_3$ accumulation at the cellular membrane results in recruitment of PDK1 (phosphoinositide-dependent kinase 1) and AKT (also known as protein kinase B; PKB), leading to AKT activation. Activated AKT controls several cellular functions such as cell survival and death by modulating the function of numerous downstream substrates. PTEN negatively regulates PI3K signalling by dephosphorylating PtdIns(3,4,5)$P_3$ to PtdIns(4,5)$P_2$ and thus mediates its tumour-suppressor function by inactivating downstream oncogenic AKT-mediated signalling[19].

In addition to its tumour-suppressor activity, PTEN was recently assigned new functions such as the maintenance of the haematopoietic stem-cell population and ovarian follicle activation[20,21]. The crucial function of PTEN in multiple cellular processes and its involvement in human diseases indicate that the enzyme needs to be tightly regulated *in vivo*. Previous studies indicated that *PTEN* is indeed regulated by multiple mechanisms at either the transcriptional or post-translational level[22,23]. At the post-translational level, PTEN function is regulated by various modifications such as phosphorylation, oxidation, *S*-nitrosylation and acetylation[23]. Ubiquitylation was also shown to regulate PTEN function, but the identity of the E3 ligase that mediates PTEN ubiquitylation is controversial. Whereas NEDD4-1 (neural precursor cell expressed, developmentally down-regulated 4) was reported as an E3 ligase for PTEN in ref. 24, this was later disputed by others[25]. In an attempt to identify the E3 ligases for PTEN, we established a 293T derivative cell line stably expressing a triple-epitope (S-protein, Flag and streptavidin-binding peptide, SBP)-tagged version of PTEN (SFB–PTEN). Tandem affinity purification using streptavidin–agarose beads and S-protein–agarose beads followed by mass spectrometry analysis enabled us to identify WWP2 as one among several PTEN-interacting proteins (Supplementary Table S1). WWP2 is an E3 ubiquitin ligase that belongs to the NEDD4-like protein family[26–29]. So far, a very limited number of substrates have been reported for WWP2, such as Oct-4 (octamer-binding transcription factor 4), RNA polymerase subunit Rpb1, the epithelial

[1]Laboratory of Cell Death & Cell Survival, Centre for DNA Fingerprinting and Diagnostics (CDFD), Nampally, Hyderabad 500001, India. [2]Mayo Clinic, 200 First Street SW, Rochester, Minnesota 55905, USA. [3]Department of Experimental Radiation Oncology, The University of Texas M. D. Anderson Cancer Center, 1515 Holcombe Boulevard, Houston, Texas 77030, USA.
[4]Correspondence should be addressed to S.M. or J.C. (e-mail: msreddy@cdfd.org.in or jchen8@mdanderson.org)

Received 1 June 2010; accepted 16 March 2011; published online 1 May 2011; DOI: 10.1038/ncb2240

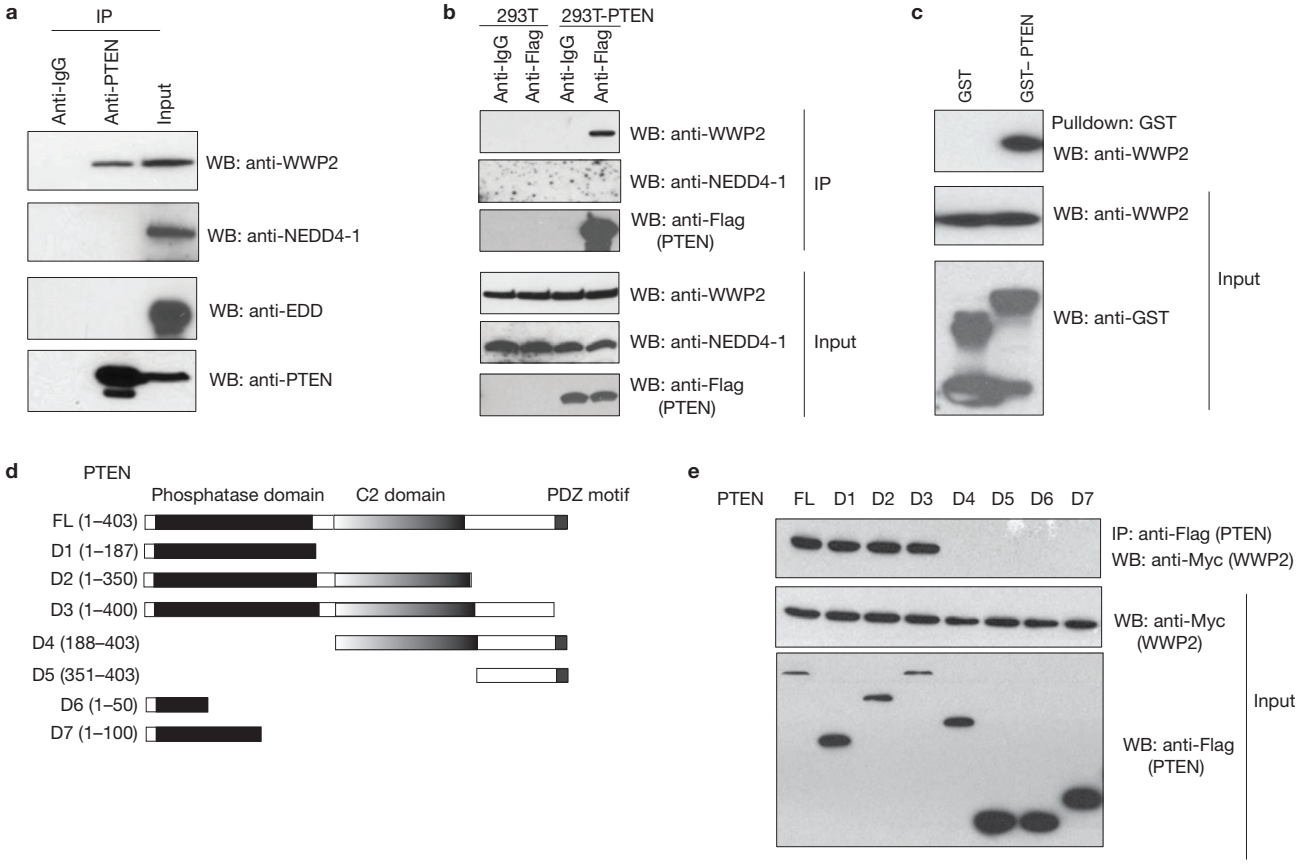


**Figure 1** WWP2 interacts with PTEN. (**a**) Immunoprecipitation (IP) using either control IgG or anti-PTEN antibody was carried out using extracts prepared from 293T cells. The endogenous interaction of WWP2, NEDD4-1 or EDD with PTEN was evaluated by immunoblotting (WB) with their respective antibodies. (**b**) Immunoprecipitation using control IgG or anti-Flag (PTEN) antibody was carried out using extracts prepared from either parental 293T cells or 293T derivative cells stably expressing Flag-tagged PTEN. The presence of WWP2 or NEDD4-1 in these immunoprecipitates was evaluated by immunoblotting with their respective antibodies. (**c**) GST pulldown assay was carried out using immobilized control GST or GST–PTEN fusion proteins on agarose beads followed by incubation with extracts prepared from 293T cells. The *in vitro* interaction of WWP2 with PTEN was assessed by immunoblotting with WWP2-specific antibodies. (**d**) Schematic representation of N-terminal Flag-tagged full-length PTEN (FL), along with its various deletion mutants (D1–D7). (**e**) 293T cells were co-transfected with the indicated Flag-tagged PTEN constructs along with those encoding Myc-tagged WWP2, and the interaction between PTEN and WWP2 was determined by immunoprecipitation and immunoblotting with the indicated antibodies. Uncropped images of blots are shown in Supplementary Fig. S4.

sodium channel and EGR-2, which are important for regulating transcription, embryonic stem-cell fate, cellular transport and T-cell activation processes[26–29].

To validate our tandem affinity purification results, we further tested the interaction of endogenous PTEN and WWP2 in cells. PTEN interacted specifically with WWP2 (Fig. 1a) but not EDD, another member of the HECT (homologous to E6AP carboxy terminus) family of E3 ligases. Although NEDD4-1 was discovered recently as an E3 ligase for PTEN (ref. 24), we did not identify NEDD4-1 in our purification (Supplementary Table S1), nor did we detect an interaction between NEDD4-1 and PTEN (Fig. 1a), which agrees with the recent report that NEDD4-1 might not be the main physiologically relevant E3 ligase for PTEN (ref. 25). We further confirmed the existence of PTEN–WWP2 complex *in vivo* by demonstrating that WWP2 co-immunoprecipitated with exogenously expressed PTEN in 293T cells (Fig. 1b). In contrast, NEDD4-1 was not seen in Flag (PTEN) immunoprecipitates (Fig. 1b). In addition, bacterially expressed glutathione *S*-transferase (GST)–PTEN pulled down WWP2 (Fig. 1c), but not NEDD4-1 (data not shown) from cell extracts, again indicating that PTEN forms a distinct complex with WWP2. PTEN has several domains that are critically important for its function. We generated expression constructs for Flag-tagged PTEN and a series of amino-terminal or carboxy-terminal deletion mutants that lack different domains (Fig. 1d). To map the WWP2-binding region on PTEN, we co-expressed these constructs along with full-length Myc-tagged WWP2. The immunoprecipitation results indicate that WWP2 interacts with the phosphatase domain of PTEN, probably within a region comprising residues 100–187 (Fig. 1e).

As WWP2 is a known HECT-domain-containing E3 ligase that regulates ubiquitin-dependent degradation of its substrates, we further assessed the significance of the PTEN–WWP2 interaction using ubiquitylation assays. HeLa cells were transiently transfected with either wild-type WWP2 or catalytically inactive WWP2$^{C838A}$ along with haemagglutinin (HA)-tagged ubiquitin. The level of PTEN ubiquitylation detected by immunoblotting after immunoprecipitation of PTEN shows that PTEN was readily polyubiquitylated by wild-type but not catalytically inactive WWP2 (Fig. 2a). To further support the idea that WWP2 mediates PTEN ubiquitylation, we carried out *in vitro* ubiquity-

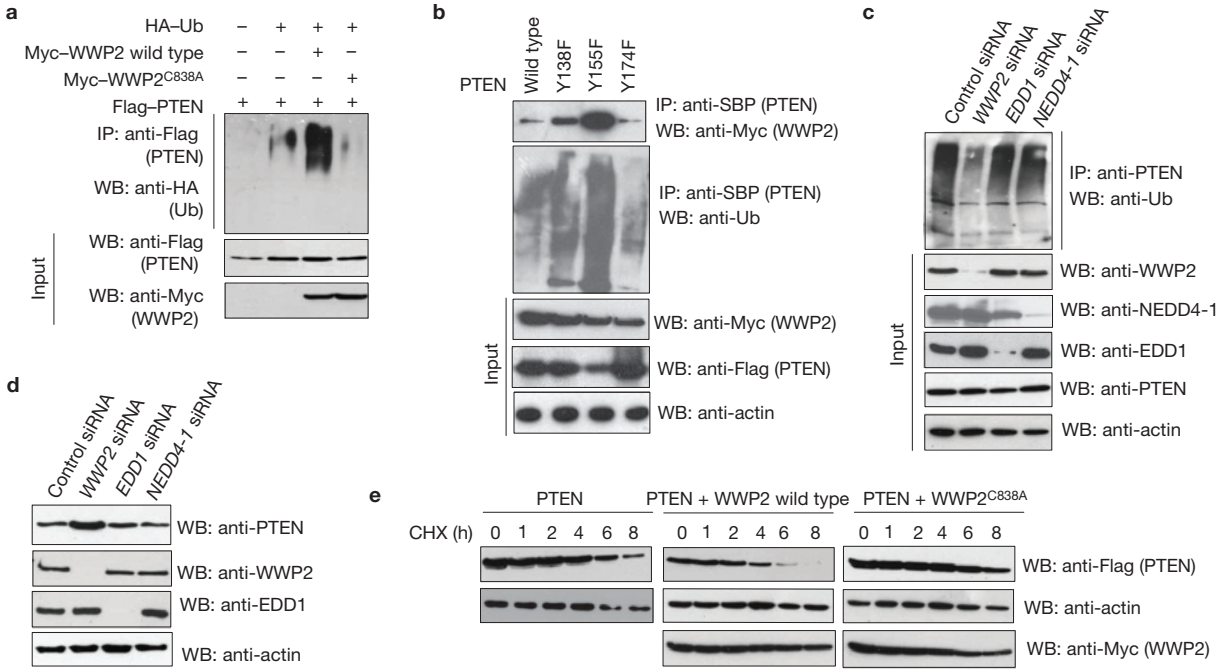


**Figure 2** WWP2 regulates PTEN protein stability by polyubiquitylation. (**a**) Myc-tagged wild-type or a catalytically inactive C838A mutant of WWP2 were expressed in HeLa cells along with Flag–PTEN and HA–ubiquitin (Ub). 24 h post-transfection, cells were treated with MG132 (10 μM) for 6 h and the levels of PTEN ubiquitylation were evaluated by immunoprecipitation of PTEN using anti-Flag antibody followed by anti-HA immunoblotting. (**b**) A triple-tagged wild-type PTEN and the PTEN tyrosine mutants along with Myc–WWP2 were expressed in 293T cells and the level of PTEN–WWP2 interaction was detected by immunoprecipitation and immunoblotting with the indicated antibodies. The level of PTEN ubiquitylation was determined by immunoblotting with anti-ubiquitin antibodies. (**c**) HeLa cells were transfected with control siRNA or siRNAs against WWP2, EDD1 and NEDD4-1. Cell lysates prepared after 6 h MG132 (10 μM) treatment were subjected to immunoprecipitaton using anti-PTEN antibodies. The ubiquitylated PTEN was detected with anti-ubiquitin antibody. The protein expression and the specificity of different siRNAs were confirmed by immunoblotting of cell extracts using antibodies as indicated. (**d**) HeLa cells were transfected with control siRNA or siRNAs against WWP2, EDD1 and NEDD4-1. The protein levels of PTEN were assessed by immunoblotting using anti-PTEN antibody. (**e**) HeLa cells transiently expressing Flag-tagged PTEN were either transfected with plasmids encoding Myc-tagged WWP2 wild type or C838A mutant. Twenty-four hours post-transfection, cells were treated with cyclohexamide (CHX) and collected at the indicated times afterwards. The protein levels of PTEN were determined by anti-Flag immunoblotting. Uncropped images of blots are shown in Supplementary Fig. S4.

lation assays using GST–PTEN as substrate in the presence of wild-type or mutant WWP2 along with the E2 ubiquitin-conjugating enzyme UbcH5b. Wild-type WWP2 but not the catalytically inactive mutant resulted in robust PTEN polyubiquitylation (Supplementary Fig. S1a).

Recently, Rak kinase was shown to regulate PTEN polyubiquitylation through tyrosine phosphorylation[30]. By modulating Rak protein levels in cells, we did not observe any significant changes in PTEN–WWP2 interaction or the PTEN protein levels (data not shown), indicating that Rak-mediated tyrosine phosphorylation might not play a role in regulating WWP2-mediated PTEN ubiquitylation. Nevertheless, several patient-derived tyrosine mutations in the PTEN phosphatase domain were reported to affect the stability of PTEN protein[31–33]. As WWP2 interacts with the PTEN phosphatase domain, we further examined these patient-derived tyrosine mutations within the WWP2-binding region. Interestingly, we found that mutation of the PTEN Tyr 155 residue significantly increased the association of WWP2 with PTEN, followed by enhanced polyubiquitylation and reduced PTEN protein levels (Fig. 2b), indicating that some yet-to-be-identified tyrosine kinases may be involved in the regulation of the WWP2–PTEN interaction.

We further evaluated endogenous PTEN ubiquitylation in cells transfected with either control short interfering RNA (siRNA) or siRNAs specific for WWP2, EDD1 or NEDD4-1 in the presence of MG132, a proteosomal inhibitor. PTEN was polyubiquitylated in the presence of intact WWP2, but its ubiquitylation was significantly reduced by the depletion of WWP2 (Fig. 2c and Supplementary Fig. S1b,c). In contrast, PTEN polyubiquitylation was unaffected in cells transfected with siRNAs against EDD1 or NEDD4-1, again indicating that WWP2 might be the predominant E3 ligase for PTEN in cells. Polyubiquitylation of PTEN by WWP2 is likely to be required for PTEN degradation, as the knockdown of WWP2 but not EDD1 or NEDD4-1 increased the steady-state levels of PTEN protein (Fig. 2d). Similar results were observed with different sets of *WWP2* siRNAs (Supplementary Fig. S1d). Moreover, in a cyclohexamide chase experiment, co-expression of Myc-tagged wild-type WWP2, but not the catalytically inactive mutant, with Flag-tagged PTEN led to diminished PTEN protein half-life (Fig. 2e). On the other hand, short hairpin RNA (shRNA)-mediated knockdown of WWP2 stabilized PTEN (Supplementary Fig. S1e). Together, these data indicate that PTEN is a substrate of WWP2.

PTEN ubiquitylation was also shown to be essential for PTEN nuclear import in addition to the regulation of its protein stability[34]. Thus, we next tested whether WWP2-mediated PTEN ubiquitylation plays a role in regulating PTEN cellular localization. Endogenous PTEN localized in both nucleus and cytoplasm, and siRNA-mediated depletion of WWP2 did not significantly affect PTEN localization (Supplementary Fig. S2a). However, in contrast to wild-type PTEN, a Cowden syndrome-associated lysine mutant of PTEN, K289R, which

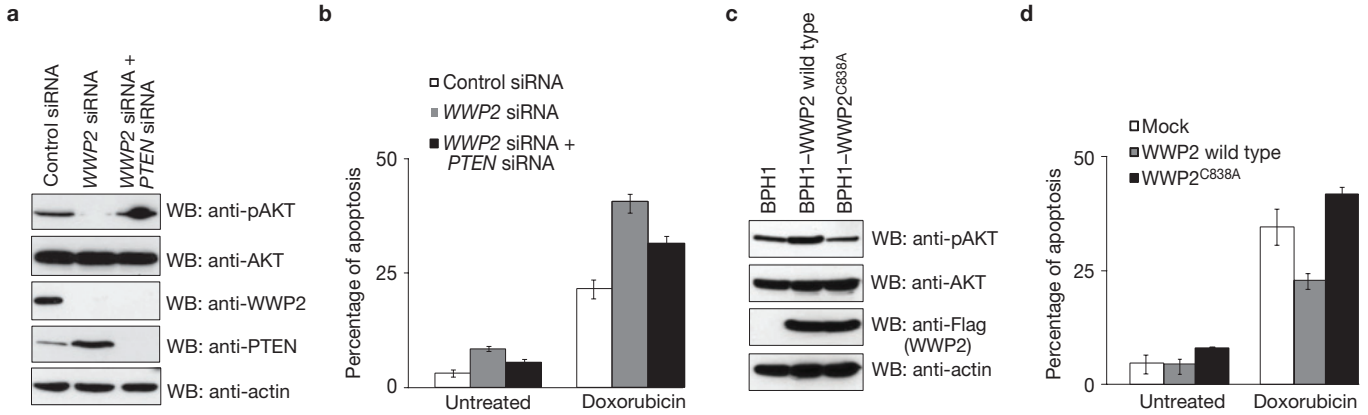


**Figure 3** WWP2 activates AKT signalling and regulates stress-induced cell death in a PTEN-dependent manner. (**a**) DU145 prostate cancer cells were transfected with either control siRNA, *WWP2* siRNA or a combination of *WWP2* siRNA and *PTEN* siRNA. 72 h after siRNA transfection, cells were lysed and cell lysates were blotted with the indicated antibodies. Activation of AKT was detected by western blotting with antibody specific to AKT phosphorylated at Ser 473 (anti-pAKT). (**b**) DU145 prostate cancer cells transfected with the indicated siRNA were either left untreated or treated with doxorubicin. The percentage of apoptotic cells was measured after 36 h of treatment by using Annexin-V staining. The data shown are derived from three independent experiments (±s.d., for doxorubicin treatment $P < 0.01$ for cells expressing *WWP2* siRNA, compared with cells expressing control siRNA or *WWP2* and *PTEN* siRNA; Student's *t*-test). (**c**) BPH1 (prostate epithelial-derived cell line) cells were transfected with either wild-type WWP2 or the C838A mutant. The cells were lysed and the activation of AKT was detected by western blotting with antibody specific to AKT phosphorylated at Ser 473 (anti-pAKT). Total AKT and expressed WWP2 proteins were detected by using AKT and Flag antibodies respectively. Actin was used as a loading control. (**d**) BPH1 cells transiently expressing wild-type or mutant WWP2 were either left untreated or treated with doxorubicin. After 36 h of treatment, apoptotic cells were determined by Annexin-V staining. The data shown are derived from three independent experiments (±s.d., for doxorubicin treatment $P < 0.05$ for cells expressing WWP2 wild-type, compared with mock treatment; Student's *t*-test). Uncropped images of blots are shown in Supplementary Fig. S4.

is also defective in ubiquitylation[34], was mainly localized in the cytoplasm (Supplementary Fig. S2b). Together, these data indicate that WWP2-mediated polyubiquitylation is mainly involved in the regulation of PTEN protein stability, whereas other E3 ligases may be responsible for PTEN subcellular localization in the cell.

As PTEN is a potent negative regulator of the PI3K–AKT pathway, we next tested whether WWP2 can regulate AKT signalling through PTEN, by using a prostate cell-line model. Indeed, knockdown of WWP2 by siRNA in DU145 cells resulted in increased endogenous PTEN protein levels and a simultaneous decrease in AKT phosphorylation with no significant effect on total AKT levels (Fig. 3a). WWP2 regulates AKT activation in a PTEN-dependent manner, because simultaneous depletion of WWP2 and PTEN by siRNA rescued AKT phosphorylation. It is well known that PTEN positively regulates stress-induced apoptosis[35,36]. As WWP2 acts as a negative regulator of PTEN, we hypothesized that loss of WWP2 might sensitize cells towards stress-induced cell death. To test this hypothesis, we depleted WWP2 by siRNA and further treated the cells with doxorubicin. Indeed, knockdown of WWP2 by siRNA sensitized DU145 cells to doxorubicin-induced apoptosis (Fig. 3b and Supplementary Fig. S3a). Further, a simultaneous depletion of WWP2 and PTEN by siRNA partially rescued the cell sensitivity towards doxorubicin-induced cell death when compared with WWP2 depletion alone (Fig. 3b). In contrast, overexpression of wild-type but not catalytically inactive WWP2 in cells derived from normal prostate epithelium (BPH1) showed increased AKT phosphorylation (Fig. 3c), followed by increased resistance to stress-induced cell death (Fig. 3d). Taken together, these results indicate that WWP2 negatively regulates stress-induced cell death, in a manner at least partly dependent on PTEN.

PTEN acts as a tumour suppressor by negatively regulating the PI3K–AKT pathway. Hence WWP2, being an E3 ligase and a negative regulator of PTEN, might function as a proto-oncogene. To test this possibility, we established DU145 cell lines with stable depletion of WWP2 using retroviral-based shRNA vectors. Consistent with our previous results, DU145-WWP2 knockdown stable clones derived from two independent shRNAs showed increased PTEN levels and decreased phosphorylated AKT when compared with control shRNA-expressing cells (Fig. 4a). Further, *WWP2* shRNA-expressing cells showed a decreased rate of cell proliferation when compared with control shRNA cells (Fig. 4b). In addition, we analysed the cell-transforming ability of WWP2 by carrying out soft-agar colony-formation assays. As shown in Fig. 4c, depletion of WWP2 markedly reduced the oncogenic capability of DU145 prostate cancer cells. We also tested the oncogenic potential of WWP2 by overexpressing WWP2 in a non-tumorigenic prostate epithelial cell line (BPH1). Stable overexpression of wild-type WWP2 resulted in reduced PTEN levels (Fig. 4d) followed by increased cell proliferation (Fig. 4e). Further, the expression of WWP2 promoted the transforming capability of normal prostate epithelial cells evident in soft-agar colony-formation assays (Fig. 4f). The transforming capability of WWP2 is dependent on its E3 ligase activity because the catalytically inactive mutant of WWP2 does not support proliferation or anchorage-independent cell growth (Fig. 4e,f). The reduced rate of proliferation and the transforming ability of *WWP2* shRNA cells were partially rescued by a simultaneous knockdown of PTEN (Fig. 4g,h; Supplementary Fig. S2d), indicating that WWP2 oncogenic potential is at least partly dependent on PTEN. Further, the tumorigenic potential of WWP2 was supported by our *in vivo* xenograft experiments. Nude mice injected with *WWP2* shRNA-expressing DU145 cells showed reduced tumour growth when compared with the control shRNA-expressing cells (Fig. 4i and Supplementary Fig. S3b). Collectively, these results indicate that WWP2 might be a potential oncogene.

Several studies have indicated that PTEN function is tightly regulated by various post-translational modifications such as phosphorylation,

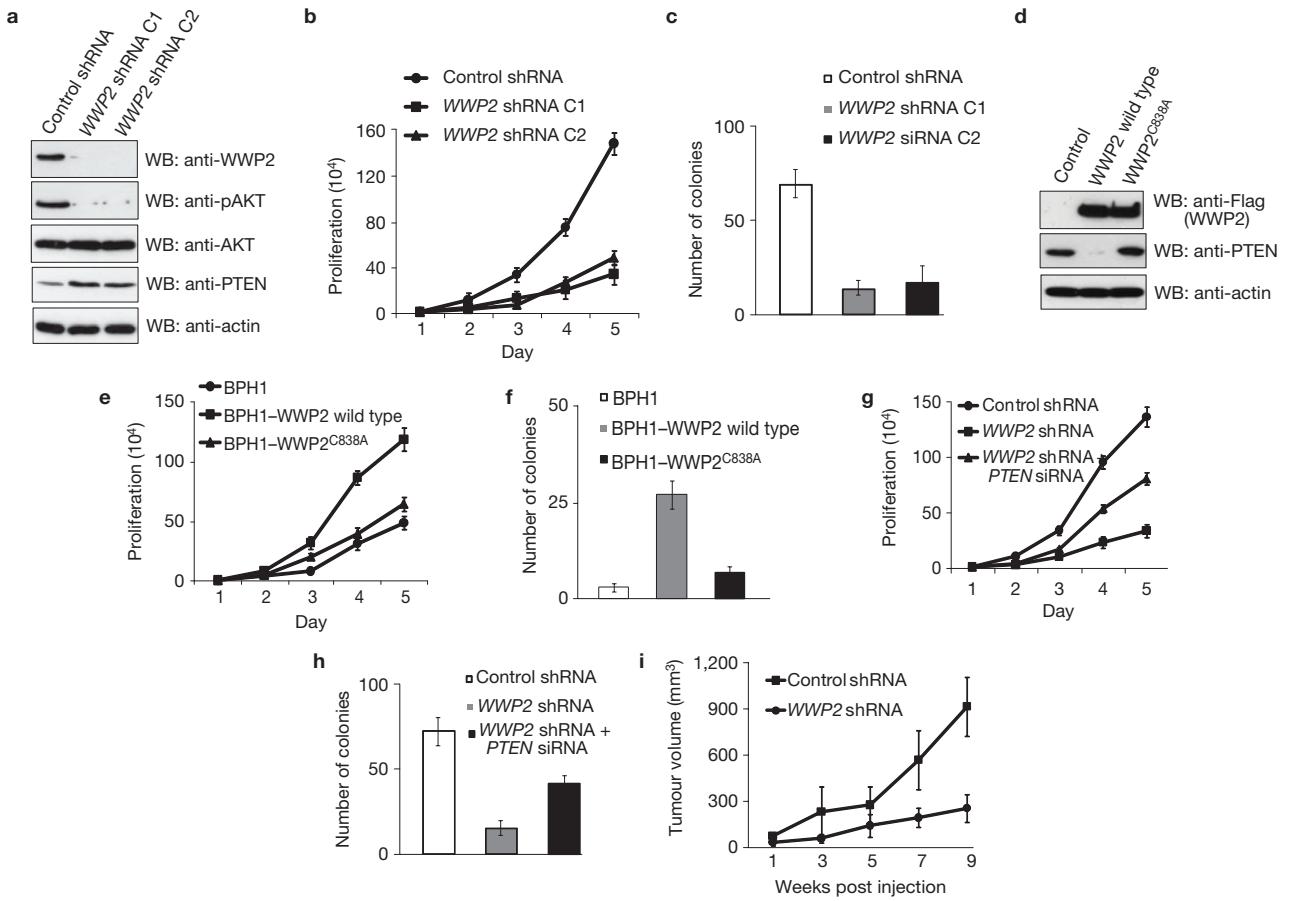


**Figure 4** WWP2 is required for tumorigenicity of cells. (**a**) DU145 cells were stably transfected with either retroviral-based control shRNA or two different *WWP2* shRNAs. The expression levels of various proteins were analysed by immunoblotting with their respective antibodies. Actin was used as a loading control. (**b**) DU145 clones stably expressing control shRNA or WWP2 shRNAs were seeded and analysed for proliferation. The data shown are derived from four independent experiments (±s.d., $P < 0.01$, compared with cells expressing control shRNA; Student's *t*-test). (**c**) DU145 cell lines stably expressing control shRNA or *WWP2* shRNA were tested for anchorage-independent growth in a soft-agar colony assay. Viable colonies after 3 weeks were counted and the data (±s.d.) from three independent experiments were presented ($P < 0.01$, compared with cells expressing control shRNA; Student's *t*-test). (**d**) Puromycin-resistant BPH1 prostate epithelial cells stably expressing either WWP2 wild type or the C838A mutant were established and the expression levels of PTEN and WWP2 were detected by the indicated antibodies. (**e**) A BPH1 parental cell line and BPH1–WWP2 wild-type or C838A mutant cells were analysed for proliferation in a similar way to that described in **b**. The data shown are derived from four independent experiments (±s.d., $P < 0.05$, compared with BPH1 parental cell line; Student's *t*-test). (**f**) A non-transformed BPH1 cell line along with WWP2 wild-type- or C838A-mutant-expressing BPH1 cells were tested for anchorage-independent growth in a similar way to that described in **c**, and the data (±s.d.) were presented as summary of three independent experiments ($P < 0.05$, compared with BPH1 parental cell line; Student's *t*-test). (**g**) DU145 stable clones expressing control shRNA or *WWP2* shRNA alone or in combination with *PTEN* siRNA were analysed for proliferation in a similar way to that described in **b**. The data shown are derived from four independent experiments (±s.d., $P < 0.01$, compared with cells expressing control shRNA; Student's *t*-test). (**h**) DU145 stable cell lines expressing control shRNA or *WWP2* shRNA alone or in combination with *PTEN* siRNA were tested for anchorage-independent growth in a similar way to that described in **c** and the data (±s.d.) were presented as a summary of three independent experiments ($P < 0.05$, compared with cells expressing control shRNA; Student's *t*-test). (**i**) Control shRNA- or *WWP2* shRNA-expressing DU145 stable cells ($5 \times 10^6$) were subcutaneously injected into nude mice and the tumour volumes were measured three times per week (±s.d., $n = 5$, $P < 0.05$, compared with cells expressing control shRNA; Student's *t*-test). Uncropped images of blots are shown in Supplementary Fig. S4.

oxidation, *S*-nitrosylation and acetylation[23]. Recent reports have also indicated that ubiquitylation plays a critical role in regulating PTEN functions[24]. However, the mechanisms and the enzymatic machinery involved in PTEN ubiquitylation are controversial and far from completely understood[25]. In this study, we have identified WWP2 as a E3 ubiquitin ligase for PTEN. We have shown that WWP2 interacts with and ubiquitylates PTEN, promoting its degradation. Interestingly, we found that the PTEN Tyr 155 residue plays a critical role in WWP2-mediated polyubiquitylation as indicated by increased association of WWP2 with PTEN, followed by enhanced polyubiquitylation and reduced PTEN protein levels with the $PTEN^{Y155F}$ mutant when compared with wild-type PTEN. As the PTEN Tyr 155 residue has been shown to be mutated in several cancers and the mutation leads to reduced protein stability[37,38], we speculate that under normal conditions PTEN is phosphorylated at the Tyr 155 residue by an as-yet-unknown kinase and thus prevents PTEN interaction with WWP2. However, in cancer cells harbouring the $PTEN_{Y155F}$ mutation, this residue can no longer be phosphorylated, which enables the interaction with WWP2 and destabilizes PTEN protein levels. In addition, treatment of cells with doxorubicin reduced the WWP2–PTEN

interaction, leading to enhanced PTEN stability (Supplementary Fig. S2c). Thus, under certain stress stimuli it is also possible that PTEN tyrosine phosphorylation could be enhanced, which may negatively affect the PTEN–WWP2 interaction and help to stabilize PTEN.

Our functional studies further indicate that WWP2 plays an important role in regulating cell death, partially in a PTEN-dependent manner by modulating the PI3K–AKT pathway. In contrast to a previous report[24], we failed to detect the interaction of PTEN with NEDD4-1 or a PTEN-associated E3 ligase activity. Although our *NEDD4-1* siRNA-mediated knockdown studies (data not shown) showed a reduced rate of cell proliferation, this might not be dependent on PTEN because we observed a similar effect of NEDD4-1 knockdown on cell proliferation in PTEN-deficient cells.

We have also uncovered a function of WWP2 as a potential oncogene. Genetic and functional studies indicated that several closely associated members of WWP2 in the HECT family of E3 ligases, such as WWP1, Itch and Smurf1/2, play crucial roles in tumorigenic processes[39]. However, so far no studies have attributed human cancers to aberrant activation of WWP2. Based on our results, WWP2 deserves further detailed investigation to fully unravel its potential in cancer development and progression. Although we identified PTEN as an important substrate of WWP2, it is certain that WWP2 has additional substrates that might also be involved in tumour progression. Our current studies are focused on identifying other functional substrates of WWP2 in tumorigenesis and extending the roles of WWP2 in other cellular processes. □

## METHODS

Methods and any associated references are available in the online version of the paper at http://www.nature.com/naturecellbiology

*Note: Supplementary Information is available on the Nature Cell Biology website*


### ACKNOWLEDGEMENTS

This work was supported in part by a grant from the Department of Biotechnology, Ministry of Science and Technology, India (to S.M.; BT/PR13134/GBD/27/202/2009), an Era of Hope Research Scholar Award (to J.C.; W81XWH-09-0409) and an NIH SPORE award (to J.N.S.; CA108961). J.C. is the recipient of an Era of Hope Scholar award from the Department of Defense (W81XWH-05-0470) and a member of MD Anderson Cancer Center (CA016672). S.K., N.R. and V.R.P. acknowledge fellowship support from the Department of Biotechnology, Council of Scientific and Industrial Research and University Grants Commission, India, respectively. S.M. is a recipient of the Department of Biotechnology's IYBA award. We also acknowledge the Institute of Life Sciences, Hyderabad, for providing basic support during some parts of this work.


### AUTHOR CONTRIBUTIONS

S.M., S.K., N.R. and V.R.P. carried out most of the experiments. J.L.P. and J.N.S. carried out the *in vivo* xenograft experiments. S.M. and J.C. designed the experiments, analysed the data and wrote the manuscript.

### COMPETING FINANCIAL INTERESTS

The authors declare no competing financial interests.


Published online at http://www.nature.com/naturecellbiology
Reprints and permissions information is available online at http://www.nature.com/reprints



1. Carnero, A., Blanco-Aparicio, C., Renner, O., Link, W. & Leal, J. F. The PTEN/PI3K/AKT signalling pathway in cancer, therapeutic implications. *Current Cancer Drug Targets* **8,** 187–198 (2008).
2. Li, J. *et al.* PTEN, a putative protein tyrosine phosphatase gene mutated in human brain, breast, and prostate cancer. *Science* **275,** 1943–1947 (1997).
3. Steck, P.A. *et al.* Identification of a candidate tumour suppressor gene, MMAC1, at chromosome 10q23.3 that is mutated in multiple advanced cancers. *Nat. Genet.* **15,** 356–362 (1997).
4. Guldberg, P. *et al.* Disruption of the MMAC1/PTEN gene by deletion or mutation is a frequent event in malignant melanoma. *Cancer Res.* **57,** 3660–3663 (1997).
5. Rhei, E. *et al.* Mutation analysis of the putative tumour suppressor gene PTEN/MMAC1 in primary breast carcinomas. *Cancer Res.* **57,** 3657–3659 (1997).
6. Wang, S. I., Parsons, R. & Ittmann, M. Homozygous deletion of the PTEN tumour suppressor gene in a subset of prostate adenocarcinomas. *Clin. Cancer Res.* **4,** 811–815 (1998).
7. Wang, S. I. *et al.* Somatic mutations of PTEN in glioblastoma multiforme. *Cancer Res.* **57,** 4183–4186 (1997).
8. Di Cristofano, A., Pesce, B., Cordon-Cardo, C. & Pandolfi, P. P. Pten is essential for embryonic development and tumour suppression. *Nat. Genet.* **19,** 348–355 (1998).
9. Kwabi-Addo, B. *et al.* Haploinsufficiency of the Pten tumour suppressor gene promotes prostate cancer progression. *Proc. Natl. Acad. Sci. USA* **98,** 11563–11568 (2001).
10. Trotman, L. C. *et al.* Pten dose dictates cancer progression in the prostate. *PLoS Biol.* **1,** E59 (2003).
11. Blumenthal, G. M. & Dennis, P. A. PTEN hamartoma tumour syndromes. *Euro. J. Hum. Genet.* **16,** 1289–1300 (2008).
12. Liaw, D. *et al.* Germline mutations of the PTEN gene in Cowden disease, an inherited breast and thyroid cancer syndrome. *Nat. Genet.* **16,** 64–67 (1997).
13. Marsh, D. J. *et al.* Germline mutations in PTEN are present in Bannayan–Zonana syndrome. *Nat. Genet.* **16,** 333–334 (1997).
14. Myers, M.P. *et al.* The lipid phosphatase activity of PTEN is critical for its tumour supressor function. *Proc. Natl. Acad. Sci. USA* **95,** 13513–13518 (1998).
15. Myers, M. P. *et al.* P-TEN, the tumour suppressor from human chromosome 10q23, is a dual-specificity phosphatase. *Proc. Natl. Acad. Sci. USA* **94,** 9052–9057 (1997).
16. Osaki, M., Oshimura, M. & Ito, H. PI3K–AKT pathway: its functions and alterations in human cancer. *Apoptosis* **9,** 667–676 (2004).
17. Paez, J. & Sellers, W. R. PI3K/PTEN/AKT pathway. A critical mediator of oncogenic signalling. *Cancer Treatment Res.* **115,** 145–167 (2003).
18. Maddika, S. *et al.* Cell survival, cell death and cell cycle pathways are interconnected: implications for cancer therapy. *Drug Resist. Updat.* **10,** 13–29 (2007).
19. Stambolic, V. *et al.* Negative regulation of PKB/AKT-dependent cell survival by the tumour suppressor PTEN. *Cell* **95,** 29–39 (1998).
20. Reddy, P. *et al.* Oocyte-specific deletion of Pten causes premature activation of the primordial follicle pool. *Science* **319,** 611–613 (2008).
21. Yilmaz, O. H. *et al.* Pten dependence distinguishes haematopoietic stem cells from leukaemia-initiating cells. *Nature* **441,** 475–482 (2006).
22. Stambolic, V. *et al.* Regulation of PTEN transcription by p53. *Mol. Cell* **8,** 317–325 (2001).
23. Wang, X. & Jiang, X. Post-translational regulation of PTEN. *Oncogene* **27,** 5454–5463 (2008).
24. Wang, X. *et al.* NEDD4-1 is a proto-oncogenic ubiquitin ligase for PTEN. *Cell* **128,** 129–139 (2007).
25. Fouladkou, F. *et al.* The ubiquitin ligase Nedd4-1 is dispensable for the regulation of PTEN stability and localization. *Proc. Natl. Acad. Sci. USA* **105,** 8585–8590 (2008).
26. Chen, A. *et al.* The HECT-type E3 ubiquitin ligase AIP2 inhibits activation-induced T-cell death by catalyzing EGR2 ubiquitination. *Mol. Cellular Biol.* **29,** 5348–5356 (2009).
27. Li, H. *et al.* WWP2-mediated ubiquitination of the RNA polymerase II large subunit in mouse embryonic pluripotent stem cells. *Mol. Cellular Biol.* **27,** 5296–5305 (2007).
28. McDonald, F. J. *et al.* Ubiquitin–protein ligase WWP2 binds to and downregulates the epithelial Na(+) channel. *Am. J. Physiol. Renal Physiol.* **283,** F431–F436 (2002).
29. Xu, H. M. *et al.* WWP2, an E3 ubiquitin ligase that targets transcription factor Oct-4 for ubiquitination. *J. Biol. Chem.* **279,** 23495–23503 (2004).
30. Yim, E. K. *et al.* Rak functions as a tumour suppressor by regulating PTEN protein stability and function. *Cancer Cell* **15,** 304–314 (2009).
31. Georgescu, M. M. *et al.* Stabilization and productive positioning roles of the C2 domain of PTEN tumour suppressor. *Cancer Res.* **60,** 7033–7038 (2000).
32. Andres-Pons, A. *et al. In vivo* functional analysis of the counterbalance of hyperactive phosphatidylinositol 3-kinase p110 catalytic oncoproteins by the tumour suppressor PTEN. *Cancer Res.* **67,** 9731–9739 (2007).
33. He, X., Ni, Y., Wang, Y., Romigh, T. & Eng, C. Naturally occurring germline and tumour-associated mutations within the ATP-binding motifs of PTEN lead to oxidative damage of DNA associated with decreased nuclear p53. *Human Mol. Genet.* **20,** 80–89 (2011).
34. Trotman, L. C. *et al.* Ubiquitination regulates PTEN nuclear import and tumour suppression. *Cell* **128,** 141–156 (2007).
35. Mayo, L. D., Dixon, J. E., Durden, D. L., Tonks, N. K. & Donner, D. B. PTEN protects p53 from Mdm2 and sensitizes cancer cells to chemotherapy. *J. Biol. Chem.* **277,** 5484–5489 (2002).
36. Zhou, M., Gu, L., Findley, H. W., Jiang, R. & Woods, W. G. PTEN reverses MDM2-mediated chemotherapy resistance by interacting with p53 in acute lymphoblastic leukemia cells. *Cancer Res.* **63,** 6357–6362 (2003).
37. Kato, H. *et al.* Functional evaluation of p53 and PTEN gene mutations in gliomas. *Clin. Cancer Res.* **6,** 3937–3943 (2000).
38. Jin, G. *et al.* PTEN mutations and relationship to EGFR, ERBB2, KRAS, and TP53 mutations in non-small cell lung cancers. *Lung Cancer* **69,** 279–283 (2010).
39. Bernassola, F., Karin, M., Ciechanover, A. & Melino, G. The HECT family of E3 ubiquitin ligases: multiple players in cancer development. *Cancer Cell* **14,** 10–21 (2008).

DOI: 10.1038/ncb2240

## METHODS

**Plasmids.** Full-length PTEN and PTEN$^{K289R}$ mutant were cloned into an S-protein/Flag/SBP triple-tagged destination vector using the Gateway cloning system (Invitrogen). Full-length WWP2 and WWP2$^{C838A}$ were also cloned into a Myc-tagged destination vector. GST-tagged PTEN, myelin basic protein (MBP)-tagged PTEN and HA-tagged ubiquitin vectors were generated by transferring their coding sequences into destination vectors using the Gateway system. The point mutants for WWP2 and PTEN were generated by PCR-based site-directed mutagenesis and verified by sequencing. Retroviral-based WWP2 wild type and C838A mutant were also generated by using the Gateway cloning system.

**Antibodies.** Rabbit anti-WWP2 antibodies were raised by immunizing rabbits with full-length GST–WWP2 fusion protein. Antisera were affinity-purified using an AminoLink Plus immobilization and purification kit (Pierce). Monoclonal anti-PTEN clone 6H2.1 (Cascade Biosciences), anti-WWP2 (1:250 dilution), anti-NEDD4-1 (1:1,000 dilution), anti-GST (1:2,000 dilution), anti-Myc (1:1,000 dilution), clone 9E10 (all from Santa Cruz Biotechnologies), anti-EDD (1:10,000 dilution; Bethyl Laboratories), anti-pAKT, anti-AKT (both 1:1,000 dilution; Cell Signaling Technology), anti-Flag, anti-actin (both 1:10,000 dilution), anti-HA (1:1,000 dilution; all from Sigma) and anti-ubiquitin (1:2,000 dilution) (Millipore) antibodies were used in this study.

**Tandem affinity purification.** PTEN-associated proteins were isolated by using tandem affinitiy purification as described before[40]. Briefly, 293T cells were transfected with SFB–PTEN and then three weeks later puromycin-resistant colonies were selected and screened for PTEN expression. The PTEN-positive stable cells were then maintained in RPMI medium supplemented with fetal bovine serum and 2 μg ml$^{-1}$ puromycin. The SFB–PTEN stable cells were lysed with NETN buffer (20 mM Tris-HCl at pH 8.0, 100 mM NaCl, 1 mM EDTA, 0.5% Nonidet P-40) containing 50 mM β-glycerophosphate, 10 mM NaF and 1 μg ml$^{-1}$ of each of pepstatin A and aprotinin on ice for 30 min. After removal of cell debris by centrifugation, crude cell lysates were incubated with streptavidin–Sepharose beads (Amersham Biosciences) for 1 h at 4 °C. The bound proteins were washed three times with NETN and then eluted twice with 2 mg ml$^{-1}$ biotin (Sigma) for 60 min at 4 °C. The eluates were incubated with S-protein–agarose beads (Novagen) for 1 h at 4 °C and then washed three times with NETN. The proteins bound to S-protein–agarose beads were resolved by SDS–polyacrylamide gel electrophoresis (SDS–PAGE) and visualized by Coommasie Blue staining. The identities of eluted proteins were revealed by mass spectrometry analysis carried out by the Taplin Biological Mass Spectrometry Facility at Harvard.

**Cell transfections, immunoprecipitation and immunoblotting.** 293T, HeLa, DU145 and BPH1 cells were transfected with various plasmids using Lipofectamine (Invitrogen) according to the manufacturer's protocol. For immunoprecipitation assays, cells were lysed with NETN buffer as described above. The whole-cell lysates obtained by centrifugation were incubated with 2 μg of specified antibody bound to either protein A or protein G–Sepharose beads (Amersham Biosciences) for 1 h at 4 °C. The immunocomplexes were then washed with NETN buffer four times and applied to SDS–PAGE. Immunoblotting was carried out following standard protocols.

**Retrovirus production and infection.** Full-length WWP2 wild type or C838A mutant was cloned into the pEF1A–HA–Flag retroviral vector using the Gateway system. Virus-containing supernatant was collected 48 and 72 h after co-transfection of pEF1A–HA–Flag WWP2 vectors and pcl-ampho into BOSC23 packaging cells, and was used to infect BPH1 cells in the presence of polybrene. Two days later, BPH1 cells were cultured in medium containing puromycin for the selection of stable clones. The clones stably expressing HA–Flag-tagged WWP2 were identified and verified by western blotting and immunostaining using anti-Flag antibodies. A similar protocol was used to generate DU145 stable cell lines that express either control shRNA or *WWP2* shRNA.

**GST pulldown and *In vitro* binding assays.** Bacterial-expressed GST–PTEN or control GST bound to glutathione–Sepharose beads (Amersham) was incubated with 293T cell lysates for 1 h at 4 °C, the washed complexes were eluted by boiling in SDS sample buffer and separated by SDS–PAGE, and the interactions were analysed by western blotting.

**RNA interference.** Control siRNA and the smart pool siRNAs against WWP2 (siRNA no. 1, 5′-UGACAAAGUUGGAAGGAAUU-3′; siRNA no. 2, 5′-GGGAGAAGAGACAGGACAAUU-3′; siRNA no. 3, 5′-CAGGAUGGGAGAUGAA-AUAUU-3′; siRNA no. 4, 5′-ACAUGGAGAUACUGGGCAAUU-3′), and the on-target individual siRNAs against EDD (ref. 40), WWP2 (siRNA no. 1, 5′-UGACAAAGUUGGAAGGAAUU-3′; siRNA no. 3, 5′-CAGGAUGGGAGAUGAA-AUAUU-3′) and NEDD4-1 (5′-GGGAAGAGAGGCAGGAUAU-3′) were purchased from Dharmacon. Prevalidated *PTEN* siRNA was purchased from Qiagen (catalogue no. SI00301504). The retroviral shRNA set for WWP2 (shRNA no. 1, 5′-AGCACAGAGUCAUUUAGAUUUA-3′; shRNA no. 2, 5′-ACCUAUGUAUUGUUUAUUUGAA-3′) was purchased from Open Biosystems. Transfection was carried out twice 30 h apart with 200 nM siRNA using Oligofectamine reagent according to the manufacturer's protocol (Invitrogen).

***In vivo* ubiquitylation assay.** HeLa cells were transfected with various combinations of plasmids as indicated in Fig. 2a along with HA-tagged ubiquitin. At 24 h post-transfection, cells were treated with MG132 (10 μM) for 6 h and the whole-cell extracts prepared by NETN lysis were subjected to immunoprecipitation of the substrate protein. The analysis of ubiquitylation was carried out by immunoblotting with anti-HA antibodies.

***In vitro* reconstitution assay.** The reactions were carried out at 30 °C for 15 min in 25 μl of ubiquitylation reaction buffer (40 mM Tris-HCl at pH 7.6, 2 mM DTT, 5 mM $MgCl_2$, 0.1 M NaCl, 2 mM ATP) containing the following components: 100 μM ubiquitin, 20 nM E1 (UBE1), 100 nM UbcH5b (all from Boston Biochem). Various combinations of WWP2 E3 ligase components as indicated were added to the reaction. MBP–PTEN bound to maltose–Sepharose beads was used as a substrate in the reaction. After ubiquitylation reaction, the Sepharose beads were washed five times with NETN buffer and boiled with SDS–PAGE loading buffer, and the ubiquitylation of PTEN was monitored by western blotting with anti-ubiquitin antibody.

**Apoptosis assays.** DU145 cells were transfected with control, WWP2, or PTEN and WWP2 siRNAs. 72 h later, transfected cells were treated with doxorubicin (1 μM, 24 h). BPH1 cells were transfected with either wild-type or mutant WWP2, and 24 h later transfected cells were treated with doxorubicin for 24 h. The apoptotic cells were then washed with PBS and stained with fluorescein isothiocyanate–Annexin V and propidium iodide according to the manufacture's protocol (BD Bioscience Annexin V Kit). Apoptotic cells (Annexin V positive, propidium iodide negative) were then determined by flow cytometry.

**Immunoflouroscence staining.** Cells grown on coverslips were fixed with 3% paraformaldehyde solution in PBS containing 50 mM sucrose at room temperature for 15 min. After permeabilization with 0.5% Triton X-100 buffer containing 20 mM HEPES at pH 7.4, 50 mM NaCl, 3 mM $MgCl_2$ and 300 mM sucrose at room temperature for 5 min, cells were incubated with a primary antibody at 37 °C for 20 min. After washing with PBS, cells were incubated with rhodamine- or fluorescein isothiocyanate-conjugated secondary antibody at 37 °C for 20 min. Nuclei were counterstained with 4,6-diamidino-2-phenylindole. After a final wash with PBS, coverslips were mounted with glycerine containing paraphenylenediamine.

**Soft-agar colony assays.** Cells were resuspended in RPMI containing 10% fetal bovine serum along with 0.5% low-melting agarose and seeded on a plate coated with 1% agarose in RPMI and 10% fetal bovine serum. Viable colonies were scored after 3 weeks of incubation and the quantified data were presented from three independent experiments.

***In vivo* xenografts.** Animal studies were carried out with previous review and approval by the Mayo Institutional Animal Care and Use Committee. Six-week-old female athymic nude mice were subcutaneously injected with $5 \times 10^6$ cells suspended in 200 μl of PBS. Starting one week after injection, tumour volumes were measured three times per week. Each cell subline was evaluated in five different animals.

**Statistical analysis.** The data are expressed as means ± s.d. from an appropriate number of experiments as indicated in the figure legends. The statistical analysis was done by using Student's *t*-test and $P < 0.05$ was considered significant.

40. Maddika, S. & Chen, J. Protein kinase DYRK2 is a scaffold that facilitates assembly of an E3 ligase. *Nat. Cell Biol.* **11,** 409–419 (2009).

nature cell biology



DOI: 10.1038/ncb2240

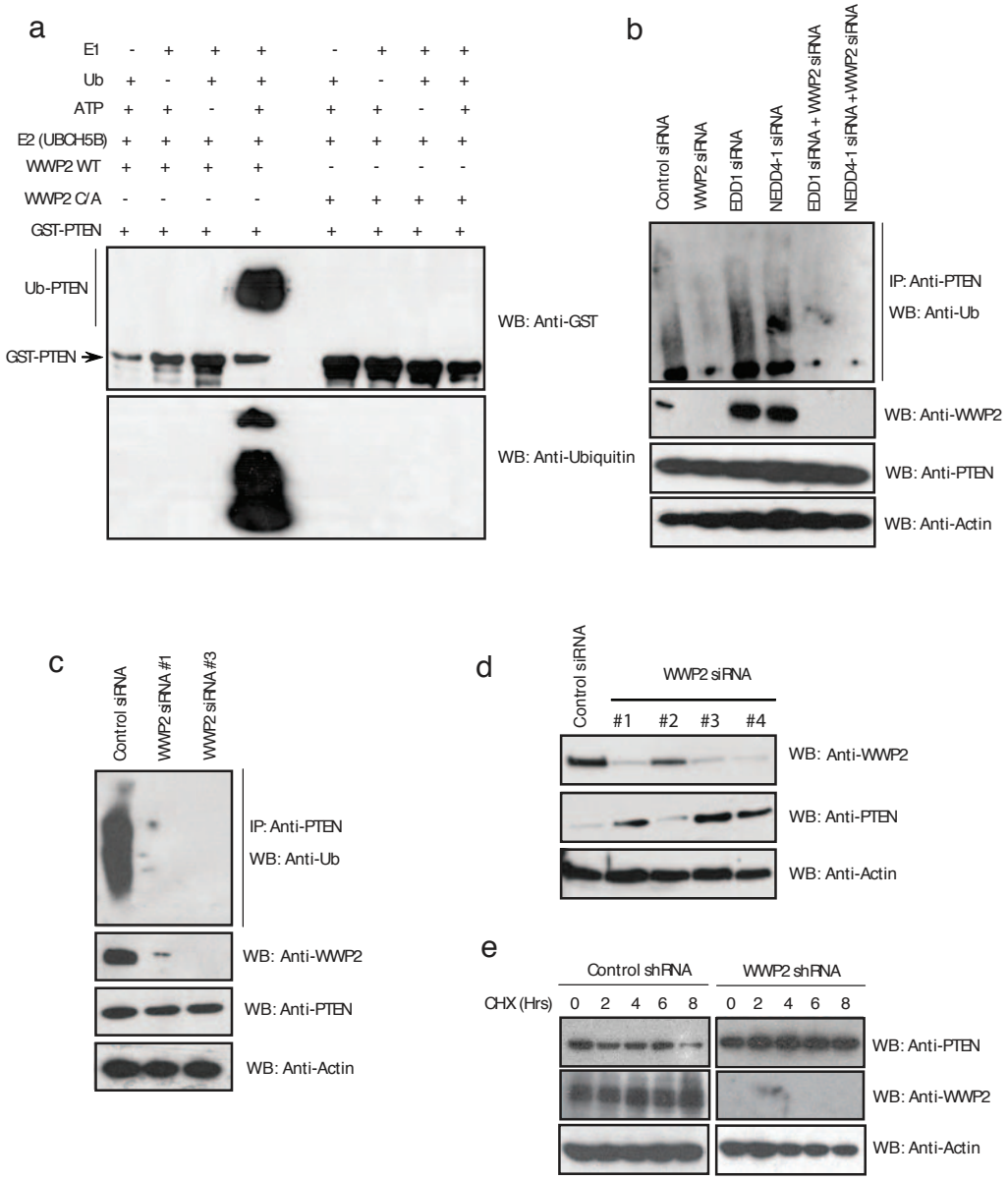


**Figure S1** (a) In vitro reconstitution experiments were performed using GST-PTEN as a substrate in the presence of recombinant ubiquitin, E1 (UBE1), E2 (UbcH5B), MBP-tagged WWP2 WT and WWP2 C/A mutant with various combinations as indicated. Ubiquitinated species of PTEN and GST-PTEN were detected by immunoblotting with anti-ubiquitin and anti-GST antibodies. (b) HeLa cells were transfected with control siRNA or siRNAs against WWP2, EDD1 and NEDD4-1. Cell lysates prepared after 6 hour MG132 (10μM) treatment were subjected to immunoprecipitaton using anti-PTEN antibodies. The ubiquitinated PTEN was detected with anti-ubiquitin antibody. (c) Cells were transfected with control siRNA or two different WWP2 siRNAs and the ubiquitinated PTEN was detected after immunoprecipitation followed by immunoblotting with anti-ubiquitin antibody. (d) HeLa cells were transfected with control siRNA or four different siRNAs against WWP2. The protein levels of PTEN were assessed by immunoblotting using anti-PTEN antibody. Actin is used as a loading control. (e) HeLa cells were transfected with either control shRNA or WWP2 shRNA and twenty four hours post-transfection, cells were treated with cyclohexamide and collected at the indicated times. The protein levels of PTEN were determined by immunoblotting.

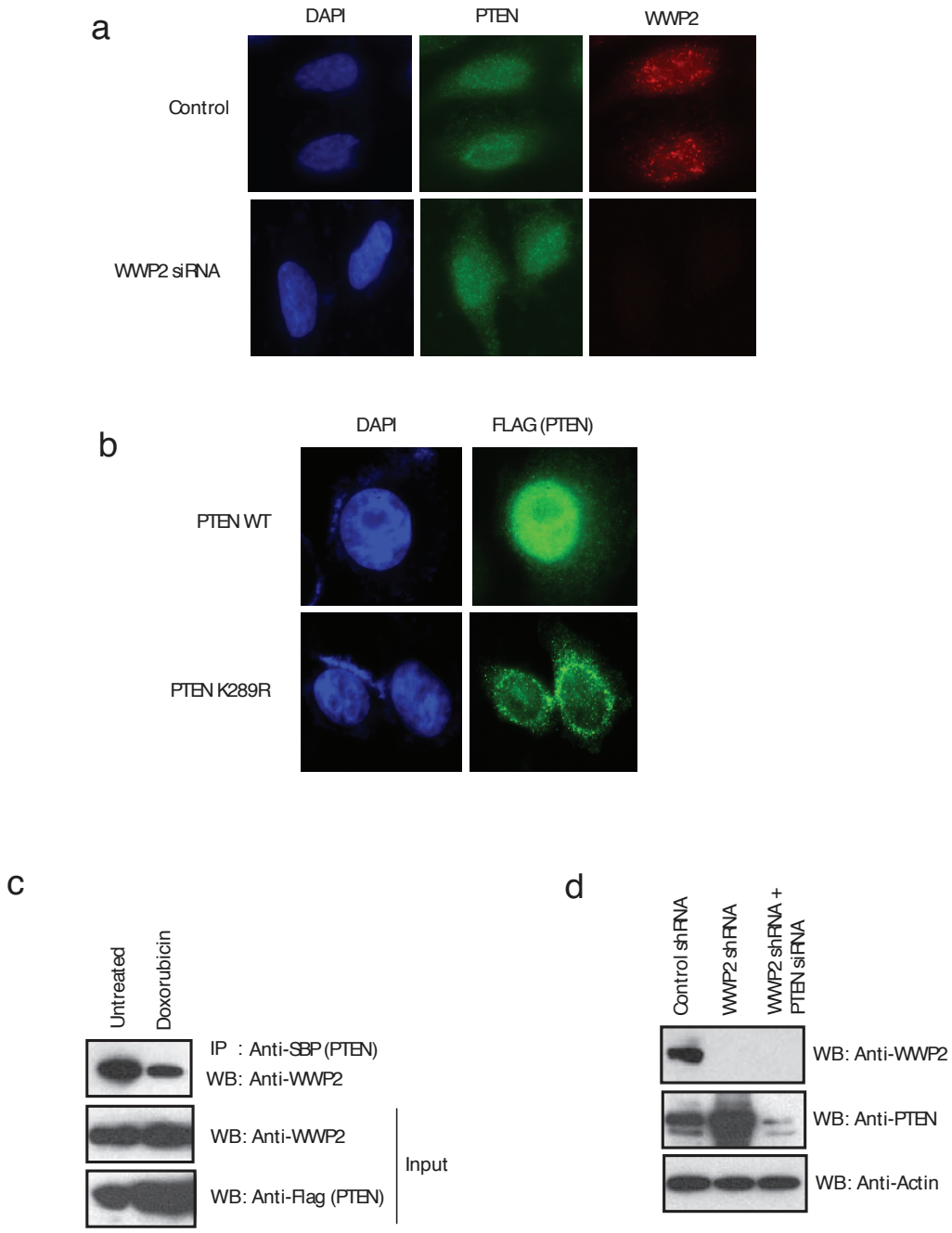


**Figure S2** (a) HeLa cells transfected with either control siRNA or WWP2 siRNA were subjected to immunofluorescence-staining using anti-PTEN and anti-WWP2 antibodies to visualize their cellular localization. (b) HeLa cells were transfected with either FLAG-epitope taggedwild type PTEN or lysine mutant K289R and the localization of PTEN was detected by immunofluorescence-staining using anti-FLAG antibody. (c) HeLa cells expressing SFB-PTEN were either left untreated or treated with Doxorubicin for 24 hours and the interaction of WWP2 with PTEN was determined by immunoprecipitation followed by immunoblotting. (d) DU145 cells were transfected with either control shRNA, WWP2 shRNA or in combination with PTEN siRNA. The expression levels of WWP2 and PTEN proteins in the were analyzed by immunoblotting with their respective antibodies. Actin was used as a loading control.

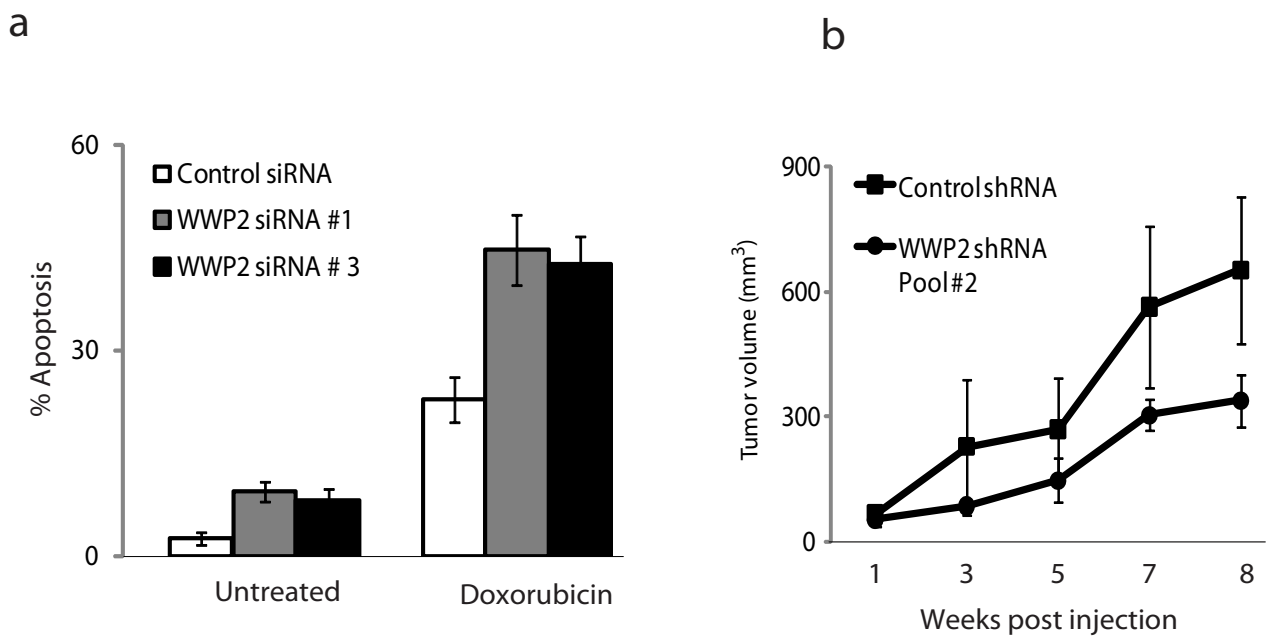


**Figure S3** (a) DU145 prostate cancer cells transfected with the indicated siRNAs were either left untreated or treated with Doxorubicin. The percentage of apoptotic cells were measured after 36 hours of treatment by using Annexin-V staining. The data shown is derived from three independent experiments (±s.d., $p<0.05$; student's t-test). (b) Control shRNA or WWP2 shRNA Pool #2 expressing DU145 stable cells ($5 \times 10^6$) were subcutaneously injected into nude mice and the tumor volumes were measured three times per week (±s.d., n=5, $p<0.05$; student's t-test).

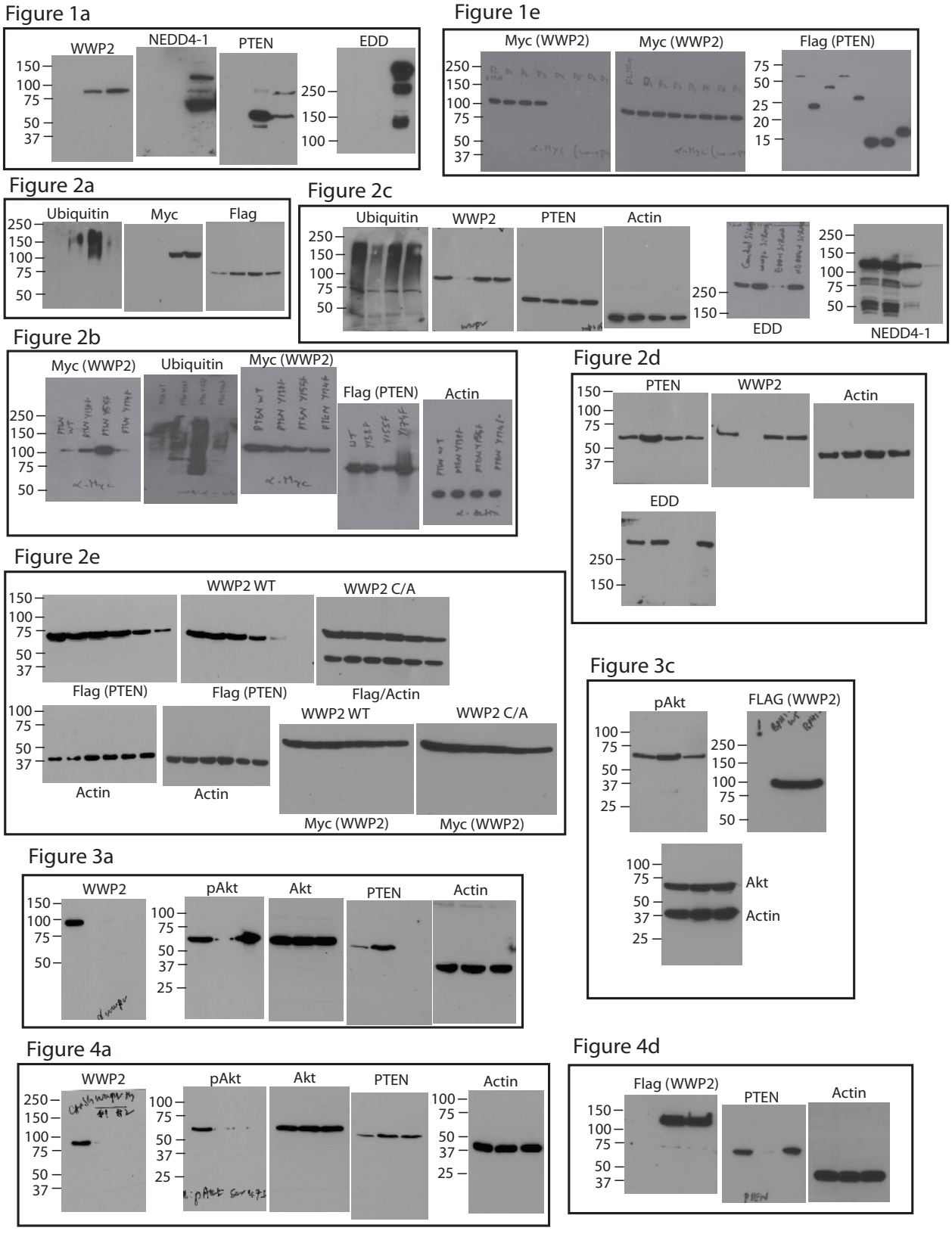


**Figure S4** Full scans of key immunoblots shown in the manuscript.

**Supplementary table 1:**

List of PTEN associated proteins identified by Mass spectrometric analysis:

| | |
|---|---|
| acetyl-coa carboxylase 1 | 103 |
| pyruvate carboxylase, mitochondrial precursor | 51 |
| propionyl-coa carboxylase alpha chain | 25 |
| propionyl-coa carboxylase beta chain | 21 |
| methylcrotonoyl-coa carboxylase beta chain | 18 |
| methylcrotonoyl-coa carboxylase subunit alpha | 18 |
| nedd4-like e3 ubiquitin-protein ligase wwp2 | 13 |
| heat shock cognate 71 kda protein | 11 |
| lipoamide acyltransferase component | 11 |
| Phosphatase and tensin homolog (PTEN) | 10 |
| acetyl-coenzyme a carboxylase alpha isoform 2 | 9 |
| heat shock protein hsp 90-alpha | 9 |
| acetyl-coa carboxylase 1 | 7 |
| heat shock 70 kda protein 1 | 7 |
| tubulin alpha-2 chain | 5 |
| heat shock 70 kda protein 1l | 4 |
| mrna encoding beta-tubulin | 4 |
| acetyl-coa carboxylase 2 | 4 |
| 78 kda glucose-regulated protein precursor | 3 |
| heat shock protein hsp 90-beta | 2 |
| heat shock-related 70 kda protein 2 | 2 |
| 2-oxoisovalerate dehydrogenase alpha subunit | 2 |
| tubulin alpha-6 chain | 1 |
| atropin-1-interacting protein 5 | 1 |
| hypothetical protein Q9hbr7 | 1 |
| heterogeneous nuclear ribonucleoprotein u | 1 |
| tubulin | 1 |
| phosphatase 1 nuclear targeting subunit | 1 |

| | |
|---|---|
| angiomotin | 1 |
| acetyl-coa carboxylase-alpha | 1 |
| c-ets-1 protein (p54) | 1 |
| heat shock 70 kda protein 6 | 1 |
| stress-induced-phosphoprotein 1 | 1 |
| class ivb beta tubulin | 1 |

THE JOURNAL OF BIOLOGICAL CHEMISTRY VOL. 286, NO. 6, pp. 4364–4370, February 11, 2011


# Angiomotin-like Proteins Associate with and Negatively Regulate YAP1*[S]

Received for publication, November 21, 2010, and in revised form, December 26, 2010 Published, JBC Papers in Press, December 27, 2010, DOI 10.1074/jbc.C110.205401

**Wenqi Wang**[‡], **Jun Huang**[§1], **and Junjie Chen**[‡2]

*From the* [‡]*Department of Experimental Radiation Oncology, The University of Texas M.D. Anderson Cancer Center, Houston, Texas 77030 and the* [§]*Life Sciences Institute, Zhejiang University, Hangzhou, Zhejiang 310058, China*

**In both *Drosophila* and mammalian systems, the Hippo pathway plays an important role in controlling organ size, mainly through its ability to regulate cell proliferation and apoptosis. The key component in the Hippo pathway is the Yes-associated protein YAP1, which localizes in nucleus, functions as a transcriptional coactivator, and regulates the expression of several proliferation- and apoptosis-related genes. The Hippo pathway negatively regulates YAP1 transcriptional activity by modulating its nuclear-cytoplasmic localization in a phosphorylation-dependent manner. Here, we describe the identification of several new PY motif-containing proteins, including angiomotin-like protein 1 (AMOTL1) and 2 (AMOTL2), as YAP1-associated proteins. We demonstrate that AMOTL1 and AMOTL2 can regulate YAP1 cytoplasm-to-nucleus translocation through direct protein-protein interaction, which can occur independent of YAP1 phosphorylation status. Moreover, down-regulation of AMOTL2 in MCF10A cells promotes epithelial-mesenchymal transition, a phenotype that is also observed in MCF10A cells with YAP1 overexpression. Together, these data support a new mechanism for YAP1 regulation, which is mediated via its direct interactions with angiomotin-like proteins.**

The control of organ (or organism) size is a fundamental question that has not been fully understood. The Hippo pathway has been identified as one of the pathways that control cell proliferation and apoptosis, both of which are essential for tissue and organ growth (1, 2). In *Drosophila*, core components of the Hippo pathway include two serine kinase proteins (Hippo and Warts) (3, 4), the mediator proteins (Fat, Expanded, and Merlin) (5–9), and the scaffold proteins (Mats and Salvador) (10, 11). Oncogene Yorkie has been identified as the main downstream target of the Hippo pathway (12). Yorkie is a transcriptional co-activator, which can bind transcription factor Sd (13) to enhance the expression of several proliferation and anti-apoptosis-related genes, including *cycE*, *diap1*, and *bantam* microRNA (11, 12, 14, 15) and therefore regulate growth and apoptosis.

The Hippo pathway is evolutionarily conserved. Mammalian orthologues of the components in the *Drosophila* Hippo pathway have been identified and found to be similarly important for cell proliferation and apoptosis (16). In mammalian cells, MST1/2 (Hippo orthologues) can be activated by several membrane receptors and subsequently phosphorylate downstream kinases LATS1/2 (Warts orthologues) in events that are coordinated by scaffold proteins MOB1 (Mats orthologue) and WW45 (Salvador orthologue) (16, 17). Activated LATS1/2 can directly phosphorylate YAP1 (Yorkie orthologue) at $Ser^{127}$, which provides a docking site for 14-3-3 protein and then leads to YAP1 cytoplasmic retention (18). Phosphorylated YAP1 also recruits Skp1/Cul1/F-box protein (SCF)-$\beta$-transducing repeat containing protein ($\beta$-TRCP) E3 ligase which promotes YAP1 ubiquitination and degradation in the cytoplasm (19). When YAP1 is in the nucleus, YAP1 binds to transcription factors such as TEA domain transcription factor (TEAD) and activates the transcription of proliferation and/or survival-related genes (20). Therefore, the Hippo pathway mainly regulates YAP1 via YAP1 phosphorylation at the $Ser^{127}$ site, which prevents YAP1 nuclear translocation and thus inhibits YAP1 function as a transcriptional co-activator. The translocation of YAP1 between cytoplasm and nucleus is very important for the control of cell proliferation and organ size (16, 17). Moreover, dysregulation of YAP1 greatly enhances tumorigenesis because YAP1 not only promotes cell proliferation but also leads to epithelial-mesenchymal transition (EMT),[3] which lessens cell contact inhibition and thus allows tumorigenesis (18, 21).

Although YAP1 phosphorylation represents a major route for YAP1 regulation, a recent study suggested that YAP may also be repressed in a phosphorylation-independent manner in *Drosophila* (22). In this case, the Hippo pathway components Expanded, Hippo, and Warts can directly bind to YAP1 through physical interaction between their corresponding PY motifs and the WW domains of YAP1. Thus, the regulation of YAP1 *in vivo* may be complex and warrant further investigation.

* This work was supported in part by the Department of Defense (DOD) Era of Hope research scholar award (W81XWH-09-1-0409) (to J. C.) and an Era of Hope Scholar award from the Department of Defense (W81XWH-05-1-0470) (to J. C.).

[S] The on-line version of this article (available at http://www.jbc.org) contains supplemental Fig. 1.

[1] To whom correspondence may be addressed. E-mail: jhuang@zju.edu.cn.

[2] To whom correspondence may be addressed: Dept. of Experimental Radiation Oncology, The University of Texas M.D. Anderson Cancer Center, 1515 Holcombe Blvd., Houston, TX 77030. E-mail: jchen8@mdanderson.org.

[3] The abbreviations used are: EMT, epithelial-mesenchymal transition; AMOTL, angiomotin-like protein; YAP, Yes-associated protein; SFB, S-FLAG-SBP; SBP, streptavidin binding peptide; TRITC, tetramethylrhodamine isothiocyanate.

Here, we report the identification of angiomotin (AMOT) and angiomotin-like proteins as new YAP1-associated proteins. AMOT is a vascular angiogenesis-related protein, which was initially identified as an angiogenesis inhibitor angiostatin-binding protein through a yeast two-hybrid screen (23, 24). AMOT can induce endothelial cell migration and tubule formation, and therefore, it promotes angiogenesis (23, 25). There are two other angiomotin-like proteins, AMOTL1 and AMOTL2. These three proteins belong to a new protein family with a highly conserved coil-coil domain, PDZ binding domain, and glutamine-rich domain (24). Just like AMOT, AMOTL1 and AMOTL2 also play important roles in cell migration and angiogenesis (26, 27), suggesting that this family of proteins may share similar functions *in vivo*.

In this study, we demonstrate that AMOT, AMOTL1, and AMOTL2 specifically interact with YAP1. This interaction is important for the regulation of YAP1 cytoplasm-to-nucleus translocation. Just like YAP1 overexpression, down-regulation of AMOTL2 in MCF10A cells promotes EMT. Together, these data suggest that YAP1 is regulated *in vivo* via its direct interactions with angiomotin-like proteins.

## EXPERIMENTAL PROCEDURES

*Antibodies*—Anti-AMOTL1, FLAG, HA, α-tubulin, and β-actin were obtained from Sigma. Anti-phospho-YAP1 ($Ser^{127}$), AKT, phospho-AKT, ERK, and phospho-ERK were purchased from Cell Signaling Technology. Anti-YAP1, Myc and GFP were obtained from Santa Cruz Biotechnology. The AMOT polyclonal antibody was raised against a glutathione *S*-transferase (GST)-AMOT (1–675 amino acids) fusion protein. AMOTL2 polyclonal antibody was raised against a Maltose binding protein (MBP)-AMOTL2 (501–780 amino acids) fusion protein. Anti-YAP1 serum was raised against GST-YAP1 full-length fusion protein. Antisera were affinity-purified using the AminoLink Plus immobilization and purification kit (Pierce).

*Plasmids*—All constructs were generated by PCR and subcloned into pDONOR201 vector using Gateway technology (Invitrogen). The entry clones were transferred subsequently into Gateway-compatible destination vectors.

PCR-mediated site-directed mutagenesis was used to generate point mutations or deletions. All these constructs include YAP1 $Ser^{127}$ to Ala mutation, YAP1 WW domain deletions (deletion of the first WW domain, WW1D, missing residues 172–203 or deletion of the second WW domain, WW2D, missing residues 232–263), and WW domain mutations (WW1m contains $Trp^{199}$ to Ala and $Pro^{202}$ to Ala mutations, WW2m contains $Trp^{258}$ to Ala and $Pro^{261}$ to Ala mutations) were verified by sequencing. Plasmids encoding FLAG-tagged wild-type AMOTL1 and two PY motif mutated constructs were kindly provided by Professor Anthony P. Schmitt (Pennsylvania State University). Plasmid encoding AMOTL2 was kindly provided by Professor Anming Meng (Tsinghua University), and the mutation of its PY motif ($Tyr^{213}$ to Ala) was created through PCR-mediated site-directed mutagenesis.

*Cell Culture and Transfection*—HeLa and 293T cells were purchased from ATCC (Manassas, VA) and maintained in DMEM medium supplemented with 10% FBS at 37 °C in 5% $CO_2$ (v/v). MCF10A cells were kindly provided from Professor Dihua Yu (M.D. Anderson Cancer Center). MCF10A cells were maintained in DMEM/F12 medium supplemented with 5% horse serum, 200 ng/ml EGF, 500 ng/ml hydrocortisone, 100 ng/ml cholera toxin, and 10 μg/ml insulin at 37 °C in 5% $CO_2$ (v/v). Cell transfection was performed using Lipofectamine 2000 (Invitrogen) following the protocol provided by the manufacturer or polyethyleneimine (Sigma).

*Establishment of Stable Cell Lines and Affinity Purification of S-FLAG-SBP (SFB)-tagged Protein Complexes*—293T cells were transfected with plasmids encoding various SFB-tagged proteins. Stable cell lines were selected by 2 μg/ml puromycin and confirmed by immunostaining and Western blotting. MCF10A cells were infected by lentivirus expressing Tet-On inducible SFB-tagged proteins, and stable pools were selected by 500 μg/ml G418 and confirmed by immunostaining and Western blotting.

For affinity purification, 293T or MCF10A cells were lysed in NETN buffer (20 mM Tris-HCl, pH 8.0, 100 mM NaCl, 1 mM EDTA, 0.5% Nonidet P-40) (with protease inhibitors) at 4 °C for 20 min. Crude lysates were centrifuged at 4 °C, 14,000 rpm for 15 min. Supernatants were incubated with streptavidin-conjugated beads (Amersham Biosciences) for 2 h at 4 °C. Beads were washed three times with NETN buffer, and bounded proteins were eluted with NETN buffer containing 2 mg/ml biotin (Sigma). Elutes were incubated with S protein beads (Novagen). Beads were washed three times with NETN buffer, and protein mixtures were subjected to mass spectrometry analysis.

*GST Pulldown Assay*—GST fusion proteins were expressed and purified from *Escherichia coli* BL21 cells. 2 μg of GST fusion proteins were immobilized on glutathione-Sepharose 4B beads and incubated with various cell lysates for 2 h at 4 °C. Beads were washed three times. Proteins bound to beads were eluted and subjected to SDS-PAGE and Western blotting analysis.

*Immunofluorescent Staining*—Cells cultured on coverslips were fixed by 4% paraformaldehyde for 10 min at room temperature and then extracted with 0.5% Triton X-100 solution for 5 min. After being blocked with 1% BSA, cells were incubated with the indicated primary antibodies for 1 h at room temperature. After that, cells were washed and incubated with FITC or rhodamine-conjugated secondary antibodies for 1 h. Cells were counterstained with 1 ng/ml DAPI for 2 min for the visualization of nuclear DNA.

*Lentivirus Packaging and Infection*—Inducible lentiviral vector and packaging plasmids (pMD2G and pSPAX2) were kindly provided by Professor Songyang Zhou (Baylor College of Medicine). Briefly, lentiviral plasmids encoding the indicated proteins were cloned into SFB-tagged lentiviral vector using Gateway technology. MCF10A cells were infected with viral supernatants with the addition of 8 μg/ml Polybrene, and stable pools were selected with medium containing 500 μg/ml G418. The expression of the indicated genes in the sta-

A

| 293T | |
|---|---|
| Bait: YAP1 | |
| **AMOT** | **54** |
| HSPA5 | 32 |
| **YAP1** | **31** |
| HSPA8 | 29 |
| ACACA | 29 |
| YWHAE | 24 |
| HSPA1A | 20 |
| TP53BP2 | 14 |
| YWHAQ | 12 |
| HSPA9 | 12 |
| MPP5 | 12 |
| WBP2 | 10 |
| **AMOTL2** | **9** |
| HSPA1L | 9 |
| LATS1 | 9 |
| **AMOTL1** | **7** |
| PTPN14 | 7 |
| HSPH1 | 7 |

| MCF10A | | | | | |
|---|---|---|---|---|---|
| Bait: YAP1 | | Bait: AMOTL1 | | Bait: AMOTL2 | |
| PTPN14 | 34 | **AMOTL1** | **32** | **AMOTL2** | **43** |
| **YAP1** | **26** | NEDD4L | 10 | TUBB2C | 16 |
| HSPA5 | 23 | HSPA8 | 8 | HSPA8 | 11 |
| **AMOTL2** | **18** | **YAP1** | **5** | ACTB | 9 |
| HSPA8 | 16 | ACTA2 | 5 | ACTA2 | 9 |
| YWHAE | 9 | HSPA5 | 3 | TUBA4A | 8 |
| **AMOTL1** | **7** | FHL2 | 3 | ATP5A1 | 7 |
| YWHAQ | 7 | NEDD4 | 3 | ACTBL2 | 6 |
| YWHAZ | 6 | HSPA9 | 2 | TUBA1C | 4 |
| TEAD1 | 5 | ETFA | 1 | HSPA9 | 4 |
| WWC3 | 5 | ACTBL2 | 1 | YWHAZ | 3 |
| YWHAG | 4 | DBT | 1 | HSPB1 | 3 |
| ALB | 4 | TUBA1C | 1 | DBT | 3 |
| TUBA1C | 3 | ACTB | 1 | GLB1 | 3 |
| HSPA1A | 3 | HYPK | 1 | TUBB1 | 3 |
| TEAD3 | 3 | HSPA7 | 1 | HSPA5 | 3 |
| YWHAB | 3 | ATP5A1 | 1 | **YAP1** | **3** |
| SFN | 3 | COPB1 | 1 | YWHAE | 3 |

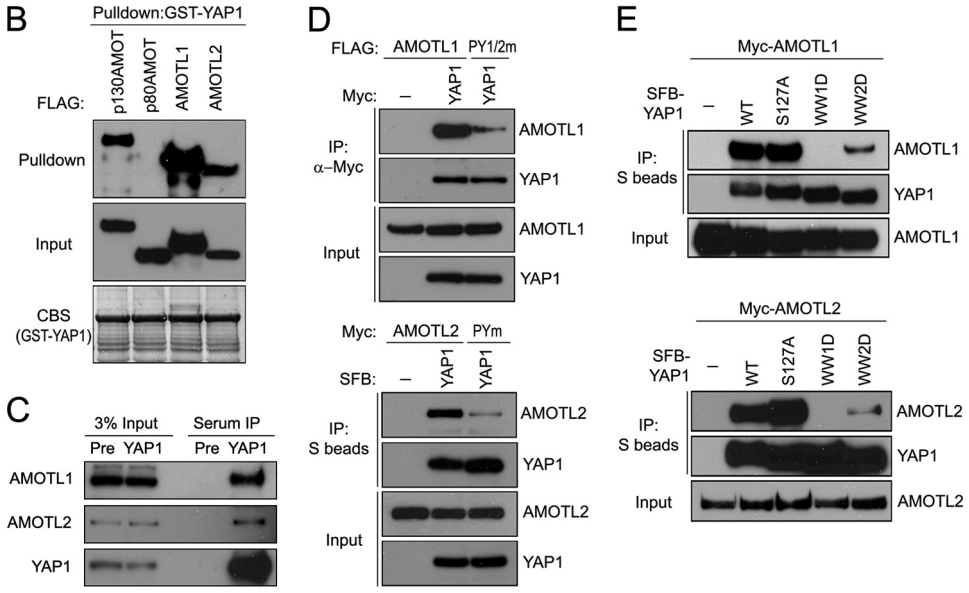


FIGURE 1. **Identification of AMOTL1 and AMOTL2 proteins as YAP1iassociated proteins in MCF10A cells.** *A*, mass spectrometry analysis revealed YAP1-associated proteins identified in 293T and MCF10A cells. AMOTL1- and AMOTL2-associated proteins were also revealed by mass spectrometry analysis in MCF10A cells. The number of peptides for each protein identified by mass spectrometry analysis was listed. *B*, GST-YAP1 fusion proteins immobilized on Sepharose beads were incubated with cell lysates containing exogenously expressed SFB-tagged p130AMOT, p80AMOT (negative control), AMOTL1, or AMOTL2. Immunoblotting was conducted using antibodies as indicated. *CBS*, Coomassie Blue staining. *C*, immunoprecipitation (*IP*) was conducted using anti-YAP1 serum or prebleed serum and lysates prepared from 293T cells. Associated endogenous AMOTL1 and AMOTL2 were revealed by immunoblotting with anti-AMOTL1 and anti-AMOTL2 antibodies, respectively. *Pre*, prebleed serum control. *D*, Myc-tagged or SFB-tagged YAP1 was used to precipitate wild-type AMOTL1/AMOTL2 or two PY motifs mutated AMOTL1 (*PY1/2m*)/PY motif mutated AMOTL2 (*PYm*) (see "Experimental Procedures"). Immunoblotting was conducted using the indicated antibodies. *E*, S protein beads were used to pull down SFB-tagged wild-type, S127A mutant, or WW domain mutant YAP1 (see "Experimental Procedures") from lysates containing exogenously expressed Myc-AMOTL1 or Myc-AMOTL2. Immunoblotting was conducted using antibodies as indicated.

ble pools was induced by the addition of 1 $\mu$g/ml doxycycline for 36 h for the experiments presented in this report.

AMOT (used as control), AMOTL1, AMOTL2, and YAP1 shRNA sets were all purchased from Open Biosystems. The target sequence for AMOT was: 5′-ggcctgtgttccactccaat-3′; for AMOTL1, 5′-ccatgagaaacaaattggaa-3′; for AMOTL2, 5′-cagtaccctcatgttgtacta-3′; and for YAP1, 5′-caggtgatactatc-aaccaaa-3′.

*Wound Healing Assay*—Confluent cells were scratched with 1-ml pipette tips, washed twice with PBS, and then incubated with the appropriate medium. 22 h later, images were captured under a microscope.

## RESULTS

*Identification of AMOT, AMOTL1, and AMOTL2 Proteins as YAP1-associated Proteins*—To identify YAP1-associated proteins, we established 293T cells stably expressing full-length YAP1 fused with an N-terminal S epitope-FLAG-SBP (streptavidin binding peptide) tag (SFB-YAP1). We performed tandem affinity purification and identified AMOT as the major YAP1-associated protein (Fig. 1*A*). To elucidate the cellular function of AMOT protein, we compared different cell lines and found that the AMOT protein level is very low in many other cell lines (such as MCF10A, HeLa, NIH3T3, and

Madin-Darby canine kidney cells) as compared with that observed in 293T cells (data not shown). We speculated that other proteins might substitute for AMOT function in these cell lines. Thus, we generated an MCF10A derivative cell line stably expressing SFB-tagged YAP1. Interestingly, we identified two other AMOT family proteins, angiomotin-like protein 1 (AMOTL1) and angiomotin-like protein 2 (AMOTL2), in this purification (Fig. 1*A*). As a matter of fact, these two proteins were also identified as YAP1-associated proteins when we performed purification in 293T cells (Fig. 1*A*). Moreover, when we conducted reverse tandem affinity purification in MCF10A cells using SFB-tagged AMOTL1 or AMOTL2, we also uncovered YAP1 as AMOTL1- or AMOTL2-associated protein (Fig. 1*A*). Together, these data indicate that AMOTL1 and AMOTL2 probably associate with YAP1 and may regulate YAP1 function in MCF10A cells.

Consistent with our purification results, both AMOTL1 and AMOTL2 interacted with YAP1, and the association between AMOTL1 or AMOTL2 with YAP1 was as strong as the AMOT/YAP1 interaction (Fig. 1*B*; please also see supplemental Fig. 1). Co-immunoprecipitation experiments further confirmed endogenous interactions between YAP1 and AMOTL1 or AMOTL2 (Fig. 1*C*).

The interaction of AMOTL1 or AMOTL2 with YAP1 was independent of YAP1 phosphorylation at the $Ser^{127}$ site (Fig. 1*E*). These interactions were mainly mediated by the first WW domain of YAP1, whereas the deletion of the second WW domain also decreased the interactions between YAP1 and AMOTL1 or AMOTL2 (Fig. 1*E*).

Because mutations in YAP1 WW domains could abolish or decrease its interaction with AMOTL1 or AMOTL2, we speculated that these interactions might be mediated by the PY motifs in these AMOT-like proteins. There are two PY motifs in AMOTL1 ($^{309}$PPPEY$^{313}$, $^{366}$PPPEY$^{370}$) and one PY motif in AMOTL2 ($^{209}$PPPQY$^{213}$). Mutating these PY motifs in either AMOTL1 or AMOTL2 dramatically decreased their interactions with YAP1 (Fig. 1*D*). Taken together, these results suggest that the interaction of AMOTL1 or AMOTL2 with YAP1 is mediated by the WW domains of YAP1 and the PY motifs in AMOTL1 or AMOL2.

*AMOTL1 and AMOTL2 Regulate YAP1 Cytoplasm-to-Nucleus Translocation*—Because AMOTL1 and AMOTL2 are cytoplasmic proteins, whereas YAP1 can shuttle between nucleus and cytoplasm, we next tested whether AMOTL1 and AMOTL2 could regulate YAP1 subcellular localization. Indeed, AMOTL1 or AMOTL2 expression resulted in the localization of endogenous YAP1- or SFB-tagged YAP1 to cytoplasm in HeLa cells (Fig. 2, *A* and *B*). Moreover, this AMOTL1- or AMOTL2-dependent cytoplasmic localization of YAP1 was blocked when we used a YAP1 mutant with deletion of its first WW domain (Fig. 2*C*). On the other hand, when the YAP1 $Ser^{127}$ phosphorylation site was mutated to Ala, AMOTL1 or AMOTL2 was still able to promote the cytoplasmic localization of this S127A mutant of YAP1 (Fig. 2*D*). These data suggest that AMOTL1 and AMOTL2 can regulate subcellular localization of YAP1, which is mediated by direct protein-protein interaction and does not require YAP1 phosphorylation at $Ser^{127}$ site.

*AMOTL2 Down-regulation Leads to EMT in MCF10A Cells*—Earlier studies demonstrated that YAP1 overexpression leads to EMT in MCF10A cells (21). Because AMOTL1 and AMOTL2 can retain YAP1 in cytosol and thus inhibit YAP1 function in the nucleus, we wondered whether down-regulation of AMOTL1 or AMOTL2 would lead to EMT in MCF10A cells.

We used lentiviral shRNAs, which efficiently targeted the down-regulation of AMOTL1 and AMOTL2 (Fig. 3*A*). RT-PCR confirmed that endogenous transcripts of AMOTL1 or AMOTL2 were respectively decreased in these stable pools (Fig. 3*B*). Although we could not detect the expression of AMOTL1 in MCF10A cells by Western blotting (data not shown), we were able to detect endogenous AMOTL2 (Fig. 3*C*) and confirmed the down-regulation of endogenous AMOTL2 protein level in these knockdown cells (Fig. 3*C*).

We noticed that cell morphology was dramatically altered in AMOTL2 stable knockdown cells, which look like spindle-shaped fibroblast cells, whereas AMOTL1 stable knockdown cells maintained epithelial morphology (Fig. 3*D*). In AMOTL2 knockdown cells, the expression of epithelial marker E-cadherin decreased and the expression of mesenchymal markers N-cadherin and vimentin increased, whereas there was no change of the expression of these markers in AMOTL1 knockdown cells (Fig. 3*E*). AMOTL2 knockdown cells also showed reduced cell-cell junction when they grew confluent, whereas AMOTL1 knockdown cells kept intact cell-cell junction (Fig. 3*F*). Moreover, AMOTL2 knockdown cells migrate faster than control MCF10A cells or AMOTL1 knockdown cells (Fig. 3*G*). All of these indicate that AMOTL2 knockdown leads to EMT in MCF10A cells.

Specifically, the EMT phenotypes observed in AMOTL2 knockdown cells were partially reversed when YAP1 expression was down-regulated at the same time (Fig. 3*H*), indicating that YAP1 is at least one of the downstream targets of AMOTL2 in this process. In addition, the nucleus-to-cytoplasm translocation of YAP1 in confluent cells was reduced (Fig. 3*I*), and YAP1 phosphorylation also decreased in AMOTL2 knockdown cells (Fig. 3*J*). Moreover, the AKT and ERK pathways were also activated in AMOTL2 knockdown cells (Fig. 3*J*), which is similar to what has been reported in cells with YAP1 overexpression (21). Together, these data suggest that down-regulation of AMOTL2 results in enhanced nuclear localization of YAP1 and EMT in MCF10A cells.

## DISCUSSION

Here, we reported the identification of several new YAP1-associated proteins, AMOT, AMOTL1, and AMOTL2. Their interactions with YAP1 are mediated by the PY motifs in AMOT-like proteins and WW domains in the central region of YAP1. Moreover, these direct protein-protein interactions are involved in the regulation of YAP1 localization and function *in vivo*. These results indicate that AMOT-like proteins belong to a new group of YAP1 regulators that may play important roles in controlling cell proliferation and contact-contact inhibition.

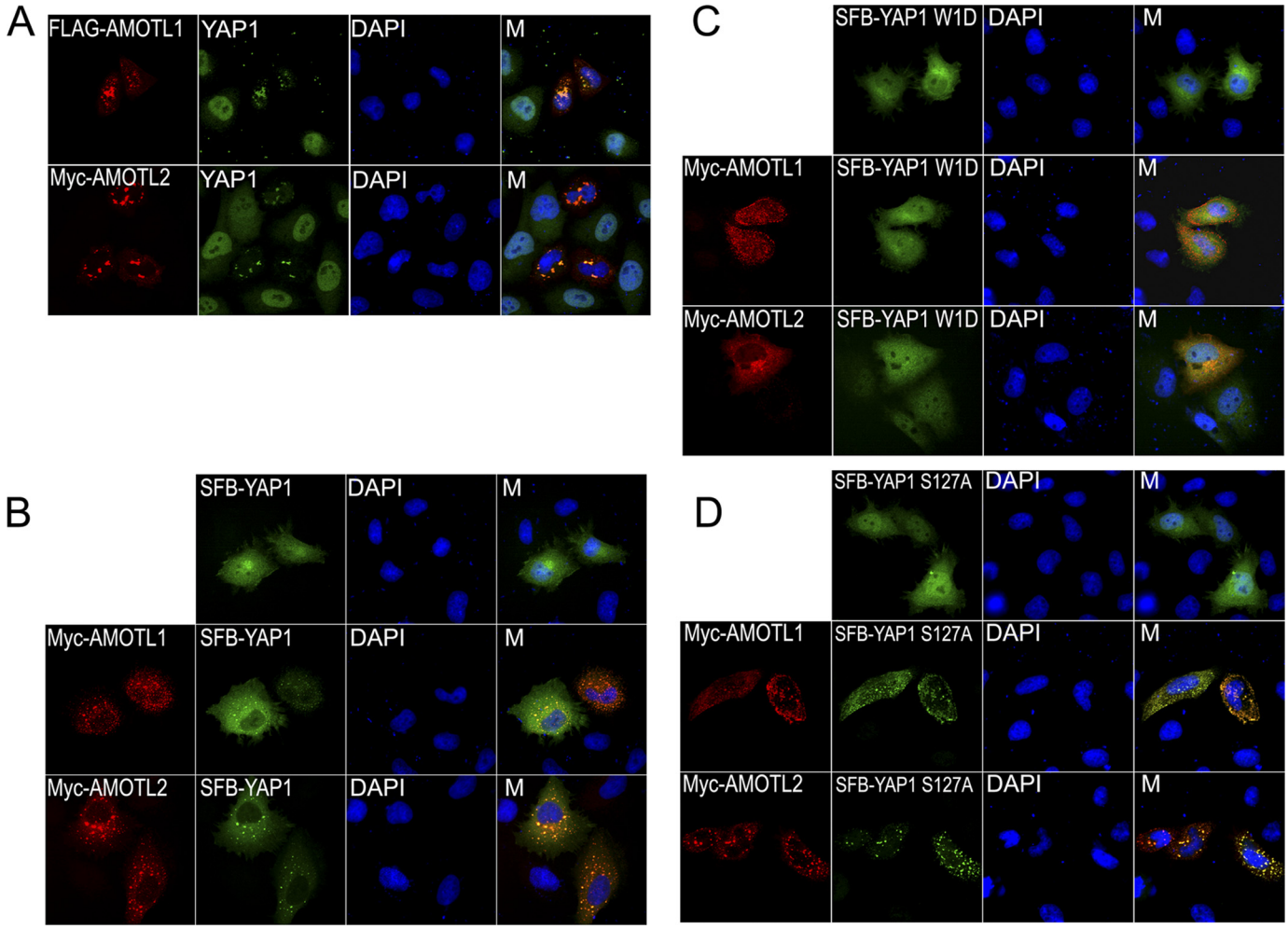


FIGURE 2. **AMOTL1 and AMOTL2 regulate YAP1 subcellular localization.** *A*, the localization of endogenous YAP1 was revealed by anti-YAP1 immunostaining in cells with or without AMOTL1 or AMOTL2 overexpression. *B–D*, HeLa cells were transfected with plasmids encoding Myc-tagged AMOTL1 or AMOTL2 with plasmids encoding SFB-tagged wild-type YAP1 (*B*), YAP1 mutant with deletion of its first WW domain (*C*), or YAP1 S127A mutant (*D*). Immunostaining was conducted using antibodies as indicated. *M*, merged.

The major regulation of YAP1 activity appears to be at its subcellular localization. The activation of the Hippo pathway leads to YAP1 phosphorylation, which promotes its cytoplasmic localization via the binding of phosphorylated YAP1 to 14-3-3 proteins in the cytosol and thus inhibits the transactivation activity of YAP1 *in vivo*. In this study, we showed that AMOT-like proteins could also keep YAP1 in the cytoplasm. In this case, the maintenance of YAP1 cytoplasmic localization does not depend on its phosphorylation status. Instead, it is mediated by direct protein-protein interaction between AMOT-like proteins and YAP1.

AMOTL1 and AMOTL2 belong to a new family of proteins including AMOT. AMOTL1 shares ~60% homologous with AMOT and has an expression pattern similar to AMOT in endothelial cell (28). We showed that just like AMOTL1 and AMOTL2, AMOT also binds directly to YAP1 via the WW domain of YAP1 and the PY motifs located at the N terminus of AMOT (please see supplemental Fig. 1). Likewise, AMOT could also mediate YAP1 cytoplasmic localization (supplemental Fig. 1*G*). Thus, all three members of this protein family behave similarly because each of them can interact with YAP1 and regulate YAP1 subcellular localization. The relative importance of these three family members in various cell lines or tissues may be determined by their expression levels. For example, AMOT expression is undetectable in MCF10A cells. Although both AMOTL1 and AMOTL2 are expressed in MCF10A cells based on RT-PCR analysis (Fig. 3*B*), we were unable to detect the expression of AMOTL1 by Western blotting (data not shown), implying that the expression of AMOTL1 may be quite low in these cells. In support of this possibility, we obtained more peptides derived from AMOTL2 than those derived from AMOTL1 from YAP1 purification in MCF10A cells (Fig. 1*A*). It is likely that this difference in protein expression may explain why down-regulation of AMOTL2 alone is sufficient to lead to deregulation of YAP1 localization and promote epithelial-mesenchymal transition in MCF10A cells (Fig. 3). It remains to be determined whether the AMOT family members may have tissue-specific expression and thus play different roles in regulating YAP1 function in various tissues or organs. Of course, it is also possible that different members of this protein family may have some distinct functions, which still needs further investigation.

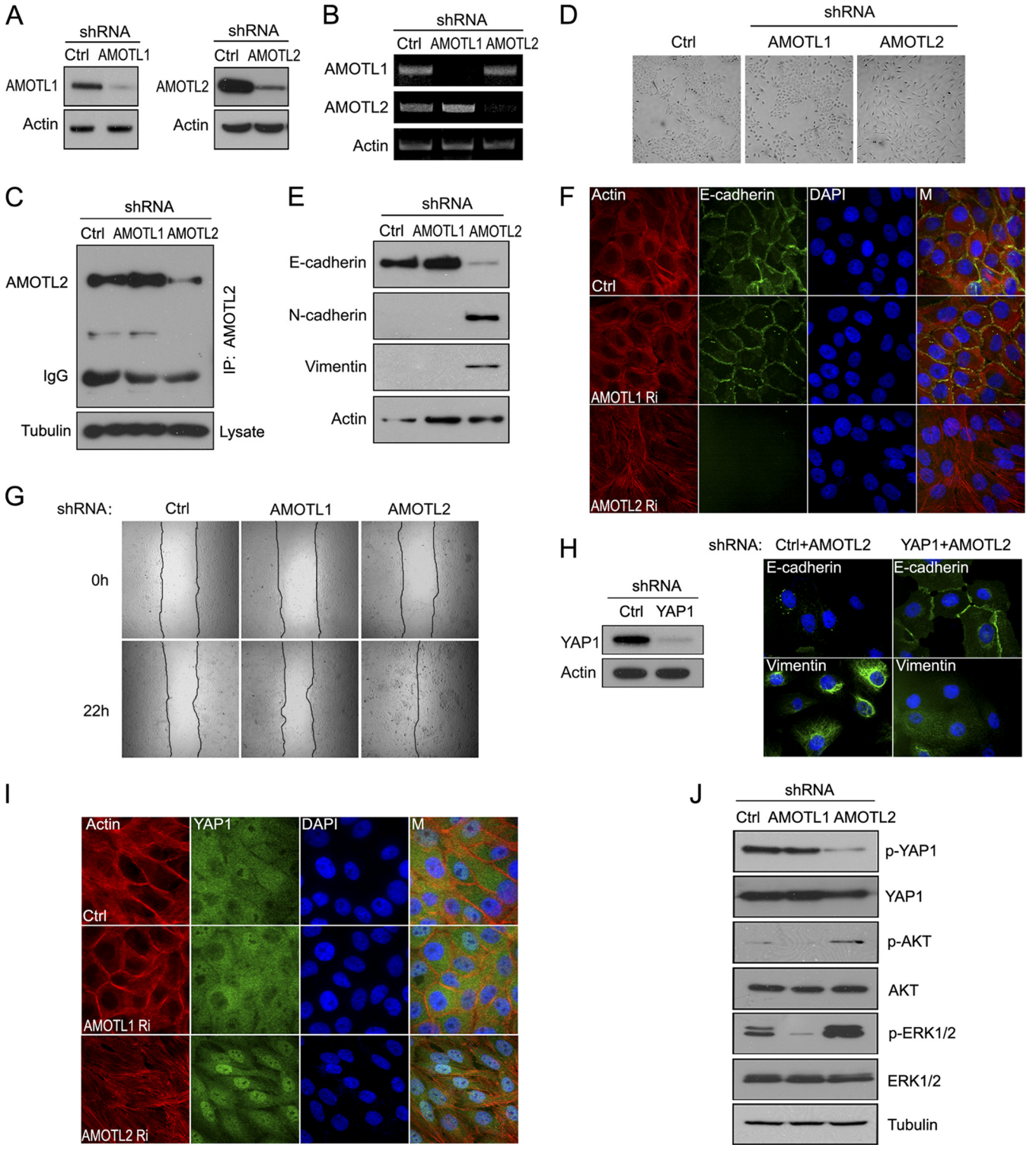


FIGURE 3. **Down-regulation of AMOTL2 causes EMT in MCF10A cells.** *A*, 293T cells were transfected with the indicated shRNAs together with plasmids encoding FLAG-tagged AMOTL1 or AMOTL2. Cells were collected 72 h later and subjected to Western blotting. *Ctrl*, control. *B*, the level of AMOTL1 or AMOTL2 transcripts was revealed by RT-PCR in the indicated stable knockdown cells. *C*, immunoprecipitation (*IP*) and immunoblotting were performed using anti-AMOTL2 serum and cell lysates prepared from the indicated cell lines. For each immunoprecipitation, a total of 1 mg of the indicated protein lysates was used. Anti-tubulin immunoblotting was included as a control. *D*, lentiviral shRNAs were used to infect MCF10A cells, and stable knockdown pools were generated. Bright field pictures were captured to reveal cell morphology in these pools. *E*, cells with AMOTL2 down-regulation displayed EMT phenotypes. E-cadherin was used as epithelial marker. N-cadherin and vimentin were used as mesenchymal markers. *F*, cell-cell junction was diminished in AMOTL2 knockdown cells. E-cadherin was used as cell-cell junction marker. Actin filaments were labeled by TRITC-phalloidin. *M*, merged. *G*, cell migration capability increased in AMOTL2 knockdown cells as determined by wound healing assay. *H*, MCF10A cells were infected with the indicated lentiviral shRNAs respectively, and stable pools were used for immunostaining with anti-E-cadherin and anti-vimentin antibodies. The efficiency of YAP1 down-regulation by shRNAs was verified by anti-YAP1 immunoblotting. *I*, YAP1 retained its dominant nuclear localization in AMOTL2 knockdown (*Ri*) cells even when cells reached confluence. *M*, merged. *J*, YAP1 phosphorylation (*p-YAP1*) decreased in AMOTL2 knockdown MCF10A cells. AKT and ERK signaling pathways were also activated in AMOTL2 knockdown cells. *p-AKT*, AKT phosphorylation; *p-ERK1/2*, ERK1/2 phosphorylation.

*Acknowledgments—We thank all colleagues in the Chen laboratory for insightful discussion and technical assistance. The M.D. Anderson Cancer Center was supported by National Institutes of Health Grant CA016672.*

## REFERENCES


1. Harvey, K., and Tapon, N. (2007) *Nat. Rev. Cancer* **7,** 182–191
2. Pan, D. (2007) *Genes Dev.* **21,** 886–897
3. Harvey, K. F., Pfleger, C. M., and Hariharan, I. K. (2003) *Cell* **114,** 457–467
4. Dan, I., Watanabe, N. M., and Kusumi, A. (2001) *Trends Cell Biol.* **11,** 220–230
5. Cho, E., Feng, Y., Rauskolb, C., Maitra, S., Fehon, R., and Irvine, K. D. (2006) *Nat. Genet.* **38,** 1142–1150
6. Bennett, F. C., and Harvey, K. F. (2006) *Curr. Biol.* **16,** 2101–2110
7. Hamaratoglu, F., Willecke, M., Kango-Singh, M., Nolo, R., Hyun, E., Tao, C., Jafar-Nejad, H., and Halder, G. (2006) *Nat. Cell Biol.* **8,** 27–36
8. McClatchey, A. I., and Giovannini, M. (2005) *Genes Dev.* **19,** 2265–2277
9. Okada, T., You, L., and Giancotti, F. G. (2007) *Trends Cell Biol.* **17,** 222–229
10. Lai, Z. C., Wei, X., Shimizu, T., Ramos, E., Rohrbaugh, M., Nikolaidis, N., Ho, L. L., and Li, Y. (2005) *Cell* **120,** 675–685
11. Tapon, N., Harvey, K. F., Bell, D. W., Wahrer, D. C., Schiripo, T. A., Haber, D. A., and Hariharan, I. K. (2002) *Cell* **110,** 467–478
12. Huang, J., Wu, S., Barrera, J., Matthews, K., and Pan, D. (2005) *Cell* **122,** 421–434
13. Goulev, Y., Fauny, J. D., Gonzalez-Marti, B., Flagiello, D., Silber, J., and Zider, A. (2008) *Curr. Biol.* **18,** 435–441
14. Nolo, R., Morrison, C. M., Tao, C., Zhang, X., and Halder, G. (2006) *Curr. Biol.* **16,** 1895–1904
15. Thompson, B. J., and Cohen, S. M. (2006) *Cell* **126,** 767–774
16. Zeng, Q., and Hong, W. (2008) *Cancer Cell* **13,** 188–192
17. Zhao, B., Lei, Q. Y., and Guan, K. L. (2008) *Curr. Opin. Cell Biol.* **20,** 638–646
18. Zhao, B., Wei, X., Li, W., Udan, R. S., Yang, Q., Kim, J., Xie, J., Ikenoue, T., Yu, J., Li, L., Zheng, P., Ye, K., Chinnaiyan, A., Halder, G., Lai, Z. C., and Guan, K. L. (2007) *Genes Dev.* **21,** 2747–2761
19. Zhao, B., Li, L., Tumaneng, K., Wang, C. Y., and Guan, K. L. (2010) *Genes Dev.* **24,** 72–85
20. Zhao, B., Ye, X., Yu, J., Li, L., Li, W., Li, S., Yu, J., Lin, J. D., Wang, C. Y., Chinnaiyan, A. M., Lai, Z. C., and Guan, K. L. (2008) *Genes Dev.* **22,** 1962–1971
21. Overholtzer, M., Zhang, J., Smolen, G. A., Muir, B., Li, W., Sgroi, D. C., Deng, C. X., Brugge, J. S., and Haber, D. A. (2006) *Proc. Natl. Acad. Sci. U.S.A.* **103,** 12405–12410
22. Ren, F., Zhang, L., and Jiang, J. (2010) *Dev. Biol.* **337,** 303–312
23. Troyanovsky, B., Levchenko, T., Månsson, G., Matvijenko, O., and Holmgren, L. (2001) *J. Cell Biol.* **152,** 1247–1254
24. Bratt, A., Wilson, W. J., Troyanovsky, B., Aase, K., Kessler, R., Van Meir, E. G., and Holmgren, L. (2002) *Gene* **298,** 69–77
25. Bratt, A., Birot, O., Sinha, I., Veitonmäki, N., Aase, K., Ernkvist, M., and Holmgren, L. (2005) *J. Biol. Chem.* **280,** 34859–34869
26. Gagné, V., Moreau, J., Plourde, M., Lapointe, M., Lord, M., Gagnon, E., and Fernandes, M. J. (2009) *Cell Motil. Cytoskeleton* **66,** 754–768
27. Huang, H., Lu, F. I., Jia, S., Meng, S., Cao, Y., Wang, Y., Ma, W., Yin, K., Wen, Z., Peng, J., Thisse, C., Thisse, B., and Meng, A. (2007) *Development* **134,** 979–988
28. Zheng, Y., Vertuani, S., Nyström, S., Audebert, S., Meijer, I., Tegnebratt, T., Borg, J. P., Uhlén, P., Majumdar, A., and Holmgren, L. (2009) *Circulation Res.* **105,** 260–270

**Supplementary Figure 1. AMOT can bind to YAP1 and regulate its subcellular localization.**

**A.** Schematic representation of human AMOT and various mutations used in this study. **B.** 293T cells stably expressing S-Flag-SBP tagged p80AMOT and N terminal AMOT were subjected to two rounds of affinity purification. Associated proteins were identified by mass spectrometry analysis. The number of peptides for each protein identified by mass spectrometry was listed in these tables. **C.** The interaction between endogenous YAP1 and p130AMOT. Immunoprecipitation experiment was performed using lysates prepared from 293T cells and pre-bleed or anti-YAP1 serum. Western blot was conducted using anti-AMOT or anti-YAP1 anti-sera. **D.** Direct interaction between YAP1 and p130AMOT. Glutathione S-transferase (GST)-YAP1 immobilized sepharose beads were incubated with cell lysates containing exogenously expressed S-FLAG-SBP tagged p130AMOT, p80AMOT or N terminal AMOT. Associated AMOT proteins were analyzed by anti-FLAG immunoblotting. **E.F.** The WW domains of YAP1 bind to the N-terminal PY motifs of p130AMOT. S protein beads were used to precipitate S-FLAG-SBP tagged wild-type or mutant YAP1 (see Experimental Procedures) or p130AMOT using lysates containing exogenously expressed HA-p130AMOT or GFP-YAP1. Western blots were performed using antibodies as indicated. **G.** AMOT-mediated sub-cellular localization of YAP1 does not require YAP1 phosphorylation at Serine 127 site. HeLa cells were co-transfected with constructs encoding SFB-tagged wild-type or S127A mutant of YAP1 with constructs encoding GFP-tagged p130AMOT. Immunostaining was performed using anti-FLAG antibody.

A

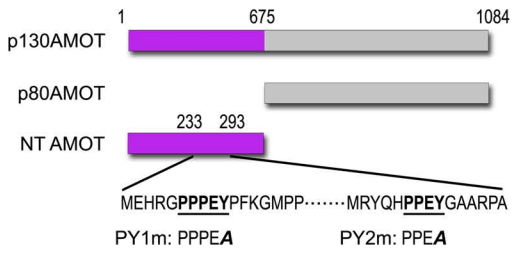


B

| Bait: p80 AMOT | |
|---|---|
| **AMOT** | **60** |
| HSPA8 | 41 |
| HSPA9 | 30 |
| HSPA5 | 25 |
| AMOTL1 | 16 |
| HSPA1A/B | 15 |
| HSPA1L | 11 |
| DYNLL1 | 9 |
| HSPA4 | 9 |
| PRDX1 | 4 |

| Bait: NT AMOT | |
|---|---|
| **YAP1** | **23** |
| **AMOT** | **22** |
| HSPA1A/B | 21 |
| STXBP4 | 18 |
| GLB1 | 15 |
| HSPH1 | 11 |
| HSPA1L | 11 |
| NEDD4 | 10 |
| TUBB2C | 9 |
| ACTB | 9 |

C

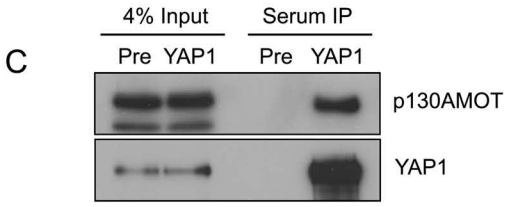


D

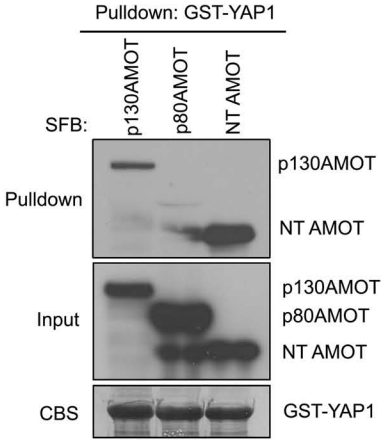


E

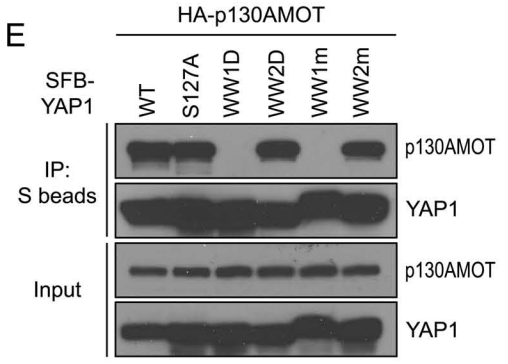


F

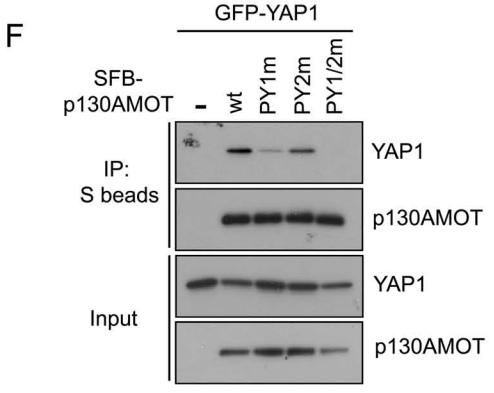


G